Article:
Morgan, H.L., Eid, N., Holmes, N. et al. (2026) Paternal over- and under-nutrition programme fetal and placental development in a sex-specific manner in mice. eLife, 15. RP109392. ISSN: 2050-084X

https://doi.org/10.7554/elife.109392

RESEARCH ARTICLE

Paternal over- and under-nutrition programme fetal and placental development in a sex-specific manner in mice

Hannah L Morgan[1,2], Nader Eid[1], Nadine Holmes[3], Matthew Carlile[3], Sonal Henson[3], Fei Sang[3], Victoria Wright[3], Marcos Castellanos-Uribe[4], Iqbal Khan[4], Nazia Nazar[4], Sean T May[4], Rod T Mitchell[5], Federica Lopes[6], Robert S Robinson[7], A Augusto Coppi[8], Vipul Batra[9], Adam J Watkins[9]*

[1]Lifespan and Population Health, School of Medicine, University of Nottingham, Nottingham, United Kingdom; [2]Maternal and Fetal Health Research Centre, Faculty of Biology Medicine and Health, University of Manchester, St Mary's Hospital, Oxford Road, Manchester, United Kingdom; [3]Deep Seq, School of Life Sciences, Queen's Medical Centre, University of Nottingham, Nottingham, United Kingdom; [4]Nottingham Arabidopsis Stock Centre (NASC), University of Nottingham, Sutton Bonington Campus, Plant Science Building, School of Biosciences, Loughborough, United Kingdom; [5]Centre for Reproductive Health, Institute for Regeneration and Repair, University of Edinburgh, Edinburgh, United Kingdom; [6]School of Medicine, University of Dundee, Dundee, United Kingdom; [7]School of Veterinary Medicine and Science, University of Nottingham, Loughborough, United Kingdom; [8]Faculty of Health and Life Sciences, University of Bristol, Bristol, United Kingdom; [9]Division of Clinical Medicine, School of Medicine and Population Health, University of Sheffield, Sheffield, United Kingdom

***For correspondence:** a.watkins@sheffield.ac.uk

Competing interest: The authors declare that no competing interests exist.

Funding: See page 20

Preprint posted
14 November 2025
Sent for Review
14 November 2025
Reviewed preprint v1
17 February 2026
Reviewed preprint v2
01 June 2026
Reviewed preprint v3
24 June 2026
Version of Record
20 July 2026

Reviewing Editor: Karen Forbes, University of Leeds, United Kingdom

eLife Assessment

This **important** study demonstrates that paternal diet influences not only testicular morphology but also placental and fetal development, supporting a role for paternal contributions to offspring health. The study also considers potential links between the microbiome and male reproductive health. By combining transcriptomic and histological analyses across multiple tissues, the evidence supporting the central conclusions of the study is **convincing**.

Abstract The association between sub-optimal paternal diet and offspring well-being is becoming established. However, the underlying mechanisms are yet to be fully defined. The aim of this study was to establish the impact of over- and under-nutrition, with or without macronutrient supplementation, on male reproductive fitness and post-fertilisation development. Male C57BL/6J mice were fed either control diet (CD), isocaloric low-protein diet (LPD), high-fat/sugar 'Western' diet (WD), or LPD or WD supplemented with methyl donors and carriers (MD-LPD or MD-WD, respectively) for 8 weeks before mating with virgin C57/BL6J females. Placental tissue was collected at embryonic day (E)8.5 to assess early placental (ectoplacental cone) morphology and metabolism and E17.5 for sex-specific transcriptomic profiling. Post-mating, stud male tissues were harvested for the assessment of testicular morphology and gene expression, gut microbiota composition, and

metabolic status. WD and MD-WD males displayed increased adiposity, hepatic cholesterol and free fatty acids, and gut microbiota dysbiosis when compared to CD-fed males. In the testes, WD and MD-WD perturbed the expression of genes associated with metabolism and transcription regulation. Additionally, we observed differential expression of multiple genes within the Wnt signalling pathway, central in the regulation of cellular proliferation, migration, survival, and cell fate determination during development. Despite no impact on fundamental male fertility, significant changes in ectoplacental cone metabolism, fetal growth, and placental gene expression were observed in response to specific dietary regimens. Interestingly, while CD male and female placentas displayed 301 genome-wide, sexually dimorphic genes, LPD, MD-LPD, WD, and MD-WD male and female placentas possessed only 13, 0, 14, and 15 sexually dimorphic genes, respectively. Our data show that while sub-optimal paternal diet has minimal impact on male fertility, fetal and placental development are perturbed in a sex-specific manner.

Introduction

Under- and over-nutrition are directly linked to poor physiological, metabolic, and reproductive health. The prevalence of poor dietary habits is increasing worldwide, with both under- and over-nutrition rising dramatically. Current estimates suggest that the combined prevalence of under- and overweight has increased in over 160 countries in both adults and school-age children (***NCD Risk Factor Collaboration (NCD-RisC), 2024***). Therefore, there has been significant interest in the impact of sub-optimal nutrition and dietary supplementation on physiological, metabolic, and reproductive health (***Jawaid et al., 2021***).

The consumption of diets high in fat and/or sugar are central to the development of various metabolic disorders, including obesity, hypertension, non-alcoholic fatty liver disease (NAFLD; also referred to as metabolic dysfunction-associated steatotic liver disease [MASLD]) (***Ludwig et al., 2001***; ***Nielsen et al., 2010***; ***von Frankenberg et al., 2017***) and metabolic syndrome (***O'Neill and O'Driscoll, 2015***, ***Saklayen, 2018***). Poor-quality diet has also been linked to impairments in fertility and reproductive fitness. Obesity has been linked to a reduction in testosterone levels, sperm concentration, motility and viability, and damage to the seminiferous tubules of the testes (***Crean et al., 2023***; ***Fan et al., 2015***; ***Leisegang et al., 2014***; ***Lotti et al., 2013***). Under-nutrition has also been linked to multiple metabolic and reproductive impairments. In rodents, a low-protein diet (LPD) significantly reduces body weight, weight of the testes, epididymis and seminal vesicles, and serum testosterone and follicle-stimulating hormone levels (***Ajuogu et al., 2020***).

Poor paternal diet also impacts negatively on fetal development and adult offspring health (***Batra et al., 2022***; ***Capobianco and Pirrone, 2023***; ***Fleming et al., 2018***). Impairments in rodent fetal and placental development have been reported in response to diets low in protein (***Morgan et al., 2021a***; ***Watkins et al., 2017***), folate (***Lambrot et al., 2013***), and high in fat (***Jazwiec et al., 2022***). Separately, children born to fathers with early-onset type 2 diabetes are leaner and have a higher insulin sensitivity than children born to healthy fathers (***Penesova et al., 2010***). Additionally, children from men with type 2 diabetes at the time of conception have a lower weight at birth, but with increased BMI in later life and a greater risk of developing type 2 diabetes and hyperlipidaemia themselves (***Moss and Harris, 2015***; ***Penesova et al., 2010***; ***Silva et al., 2017***). In rodent models, paternal high-fat and -sugar diets perturb offspring insulin and glucose homeostasis (***César et al., 2022***), behaviour, and gut microbiota composition (***Bodden et al., 2022***). Interestingly, poor paternal diet impacts on offspring health in a sex-specific manner. Sex-specific changes in offspring tissue lipid abundance have been reported following a paternal LPD (***Furse et al., 2023***; ***Morgan et al., 2022***; ***Morgan et al., 2020b***; ***Watkins et al., 2018***). Similarly, paternal high-fat diet in rats programmes pancreatic β-cell dysfunction and impaired glucose metabolism in female offspring (***Ng et al., 2010***) and adult-onset obesity in males (***Sanchez-Garrido et al., 2018***).

Separate from macronutrient modification, the significance of dietary micro-nutrients, such as vitamins, minerals, and antioxidants, has also been assessed. Studies have focused on supplementation as a potential means to reverse or alleviate the effects of sub-optimal diets. In rats, the detrimental effects of a high-fat/sucrose diet on liver steatosis were ameliorated through the supplementation with a range of methyl donors and carriers such as folate, choline, betaine, and vitamin B12 (***Cordero et al., 2013a***; ***Cordero et al., 2013b***). In mice, supplementing calorically restricted males with

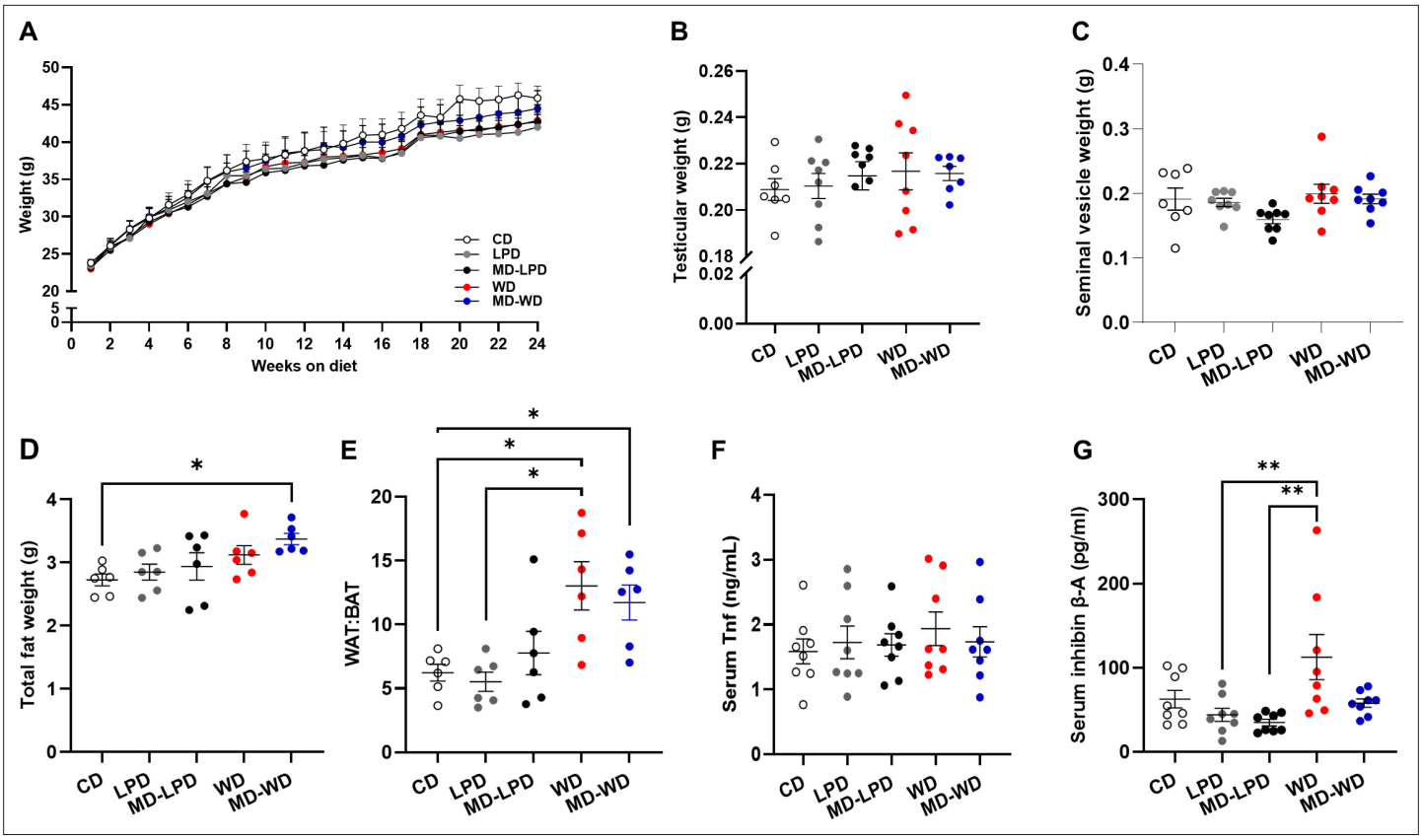

Figure 1. Impact of diet on male growth. (**A**) Mean weekly body weight of males fed either a control diet (CD), low-protein diet (LPD), methyl donor-supplemented LPD (MD-LPD), Western diet (WD), or methyl donor-supplemented Western diet (MD-WD). Mean (**B**) testicular weight, (**C**) seminal vesicle weight, (**D**) total fat weight (combined weight of individual fat pads), and (**E**) ratio of white adipose tissue (WAT) to brown adipose tissue (BAT). Mean serum (**F**) Tnf and (**G**) inhibin β-A chain levels. *N*=6–8 males in each group. Data are presented as mean ± SEM and were analysed using a one-way ANOVA with Holm-Sidak post hoc tests for multiple comparison. *p<0.05, **p<0.01.

vitamins and antioxidants prevented sperm oxidative damage and normalized offspring growth and adiposity (***McPherson et al., 2016***). Similarly, supplementation of a paternal LPD with methyl donors and carriers has been shown to normalise patterns of fetal overgrowth in mice (***Morgan et al., 2020a***).

While the association between paternal diet and offspring well-being is becoming established, the underlying mechanisms are yet to be fully defined. The aim of this study was to establish and compare the impact of over- and under-nutrition on male reproductive fitness and post-fertilisation development. As poor micronutrient status has also been associated with perturbed fetal development (***Lambrot et al., 2013***), we additionally explored the role that supplementation with specific methyl donors and carriers may play in ameliorating any detrimental effects of poor paternal diet.

Results

Male physiology and metabolic status

To investigate the impact of over- and under-nutrition, with or without methyl donor and carrier supplementation, on male reproductive fitness, we fed male C57BL/6J mice one of five diets comprising a control diet (CD), LPD, LPD supplemented with methyl donors (MD-LPD), Western diet (WD), or WD supplemented with methyl donors (MD-WD) for up to 24 weeks. Over the course of the feeding period, all experimental groups became lighter than CD males (***Figure 1A***). However, no significant differences were observed when analysed at individual time points or as average growth profile (area under the growth curve). At the time of cull, there was no difference in mean testicular (***Figure 1B***) or seminal vesicle (***Figure 1C***) weights. MD-WD had an increased total fat mass (combined weight of gonadal, peri-renal, inguinal, and interscapular fat pads) when compared to CD-fed males

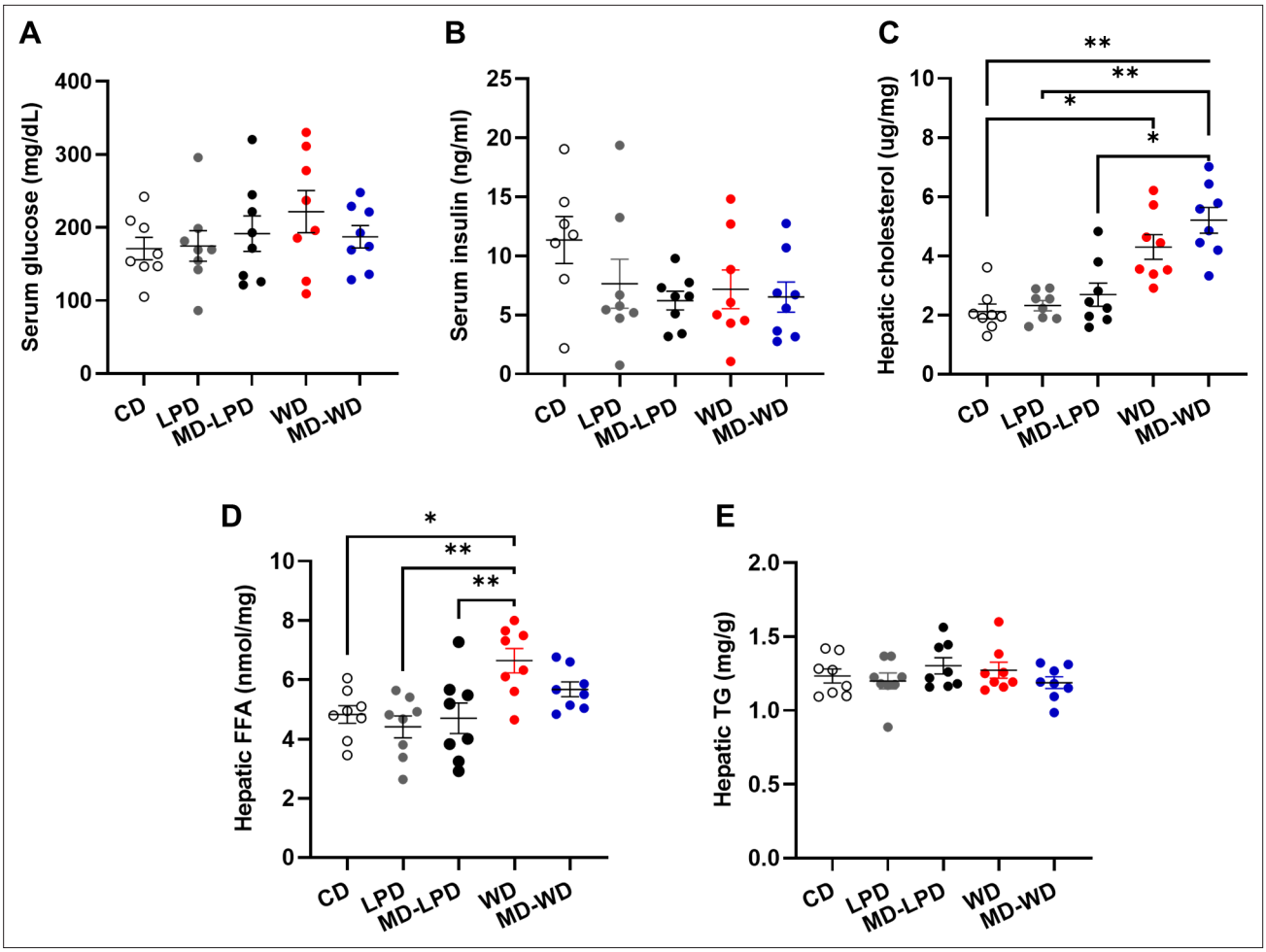

Figure 2. Impact of diet on male non-fasting metabolic status. Serum (**A**) glucose and (**B**) insulin in males fed either a control diet (CD), low-protein diet (LPD), methyl donor-supplemented LPD diet (MD-LPD), Western diet (WD), or methyl donor-supplemented WD (MD-WD). Hepatic (**C**) cholesterol, (**D**) free fatty acids (FFAs), and (**E**) triglyceride (TG) concentrations. *N*=8 males in each group. Data are presented as mean ± SEM and were analysed using a one-way ANOVA with Holm-Sidak post hoc tests for multiple comparison. *p<0.05, **p<0.01.

(***Figure 1D***, p=0.01). Analysis of white (WAT, combined weight of gonadal, peri-renal, and inguinal fat) to brown adipose tissue (BAT; interscapular) ratio revealed an increase in WD and MW-WD males when compared to CD-fed males (***Figure 1E***, p<0.05). Next, we assessed serum profiles of central indicators of inflammatory status (Tnf) and testicular regulation (inhibin β-A chain). There was no difference in the concentrations of Tnf (***Figure 1F***) between males. However, WD-fed males displayed an elevated concentration of serum inhibin β-A chain, a paracrine regulator of germ cell proliferation, spermatogenesis, and Leydig cell steroidogenesis, when compared to LPD- and MD-LPD-fed males (***Figure 1G***, p<0.01).

As we observed significant changes in adiposity in response to our diets, we assessed stud male metabolic status. There were no differences in the concentrations of serum glucose (***Figure 2A***) or insulin (***Figure 2B***) between groups. In contrast, WD males displayed an elevated concentration of hepatic cholesterol when compared to CD males (***Figure 2C***) while MD-WD males displayed elevated levels when compared to CD, LPD, and MD-LPD males (***Figure 2C***, p<0.05). WD males also displayed elevated levels of free fatty acids (FFAs) when compared to CD, LPD, and MD-LPD males (***Figure 2D***, p<0.05), while the levels of FFA in MD-WD males was not significantly different to that of either CD or WD males. No differences in the concentration of hepatic triglyceride were observed between groups (***Figure 2E***).

Analysis of gut bacterial profiles revealed no difference in overall bacterial diversity (***Figure 3A***) or species evenness (***Figure 3B***) between groups. When analysed at the phylum level (***Figure 3C***),

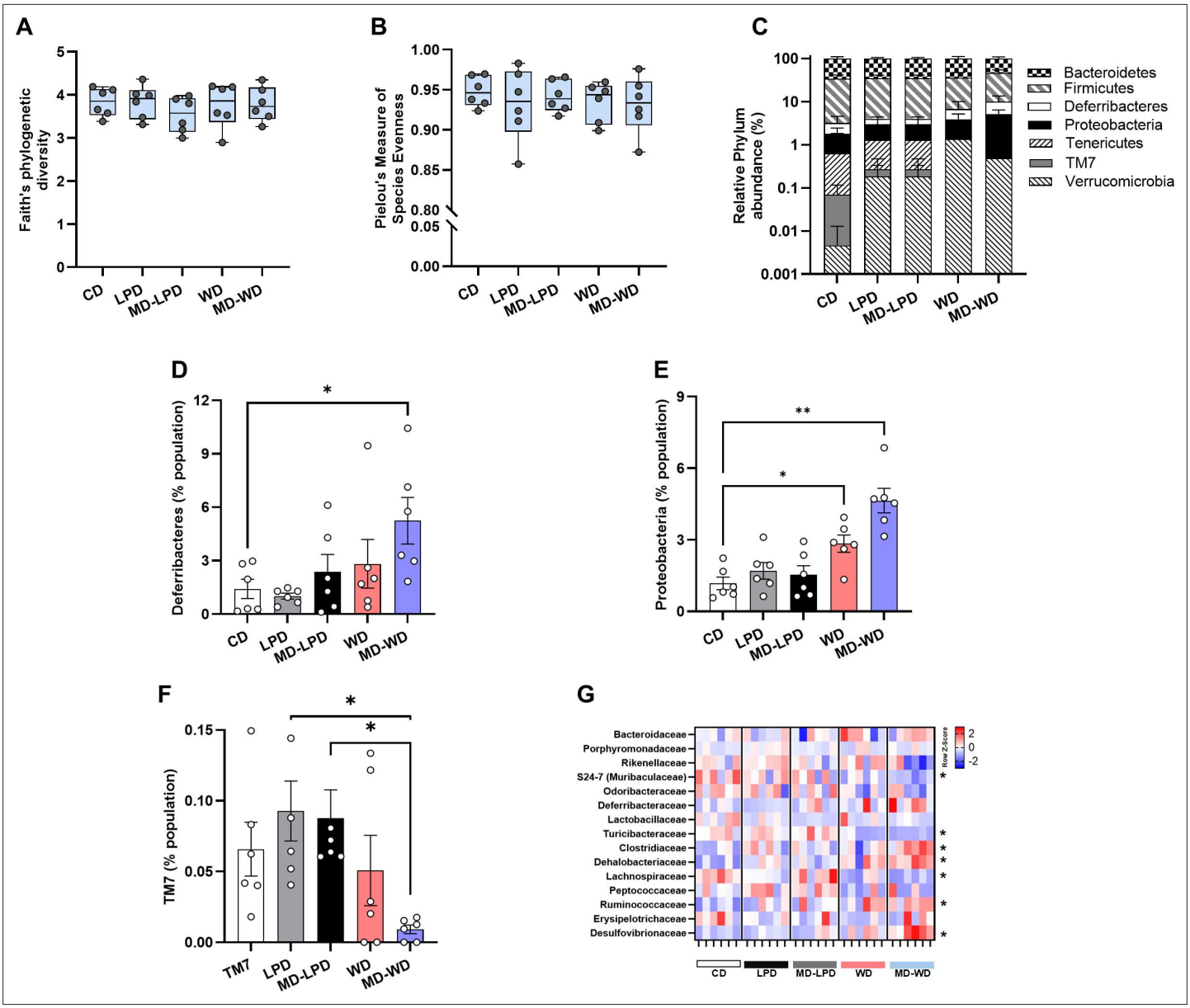

Figure 3. Impact of diet on male gut microbiota. (**A**) Faith's phylogenetic diversity and (**B**) Pielou's measure of species evenness. (**C**) Overall bacterial abundance at the phylum level and relative abundance of (**D**) Deferribacteres, (**E**) Protobacteria, and (**F**) TM7 phylum. (**G**) Relative (Z-score) abundance of bacteria at the family level in males fed either a control diet (CD), low-protein diet (LPD), methyl donor-supplemented LPD diet (MD-LPD), Western diet (WD), or methyl donor-supplemented WD (MD-WD). *N*=8 males in each group. Data are presented as box plots in A, showing trhe mean (solid line) and 95% data ranges, and as mean ± SEM in C–F. Data were analysed using either a one-way ANOVA (panels **D**, **E**, **F**, and **G**) or Kruskal-Wallis test (panels **A**, **B**, and **C**) with Holm-Sidak or Dunn's post hoc tests for multiple comparison, respectively. *p<0.05, **p<0.01.

MD-WD males displayed a significant increase in the abundance of Deferribacteres (***Figure 3D***; p=0.042), while WD and MD-WD males displayed an increased abundance of Proteobacteria (***Figure 3E***; p<0.05) when compared to CD males. Furthermore, the abundance of TM7 (Saccharibacteria) was decreased in MD-WD males when compared to LPD- and MD-LPD-fed males (***Figure 3F***; p<0.05). Analysis of bacteria at the family level identified significant reductions in the abundance of Turicibacteraceae and Lachnospiraceae in both WD and MD-WD males when compared to CD-fed males (***Figure 3G***, p<0.05). Additionally, the abundance of S24-7 (Muribaculaceae), Clostridiaceae, Dehalobacteriaceae, Ruminococcaceae, and Desulfovibrionaceae were all significantly altered (both increased and decreased) in MD-WD males when compared to CD males (***Figure 3G***; p<0.05).

Sub-optimal diet alters seminiferous tubule cytoarchitecture and cellular distribution

As diet and nutritional status have been directly linked to reproductive health, we next assessed testicular and epididymal morphology. Gross histological analysis (***Figure 4A***) of testicular tissue revealed an increased number of tubules displaying abnormalities such as vacuoles, loss of the epithelium, or complete loss of the tubular architecture (***Figure 4B***) in WD and MD-WD males when compared to CD, LPD, and MD-LPD males (***Figure 4C***, $p<0.01$). To analyse seminiferous tubule composition further, we stained testicular sections from the same males to determine Sertoli (Sox-9), spermatocytes and spermatids (Ddx4), and spermatogonial stem (Plzf) cells (***Figure 4D***) numbers. There were no differences in the mean number of nuclei per tubule (as determined via DAPI staining; ***Figure 4E***), the number of Sertoli cells per tubule (***Figure 4F***) or the number of spermatocytes and spermatids per tubule (***Figure 4G***). However, a significant reduction in the number of $Plzf^+$ spermatogonial stem cells was detected in tubules from LPD and WD males when compared to CD males (***Figure 4H***, $p<0.05$). In contrast, no difference in the number of $Plzf^+$ cells were observed in MD-LPD and MD-WD testes when compared to CD males (***Figure 4H***).

Testicular gene expression is perturbed in a diet-specific manner

To define the impact of diet on testicular gene expression profiles, we performed a micro-array transcriptomic analysis using testicular tissue from the same males. We identified 0, 0, 402 (267 downregulated, 135 upregulated) and 285 (187 downregulated, 98 upregulated) differentially expressed (fold change <–1 or >1; padj<0.05) genes in LPD, MD-LPD, WD, and MD-WD testes when compared to CD testes (***Figure 5A–C and F***). In WD testes, we identified 267 downregulated and 135 upregulated genes (***Figure 5C***) associated with an upregulation of fatty acid metabolism (GO:0006631) and a downregulation of chromatin binding (GO:0003682), RNA binding (GO:0003723), and actin filament organization (GO:0007015) pathways (***Figure 5D***). Network analysis of the 402 differentially expressed genes within the WD testes identified several modular relationships between genes (***Figure 5E***). Specifically, we observed significant (padj<0.05) gene nodes associated with the expression of *Ywhae* (FC –1.14), *Rara* (FC –1.35), *Dnmt1* (FC –1.36), *H3f3a* (FC 1.12), and *Wdr5* (FC –1.3). In MD-WD testes, we identified 187 downregulated, 98 upregulated genes (***Figure 5F***) associated with an upregulation of RNA splicing (GO:0008380) and RNA binding (GO:0003723), and a downregulation of DNA damage (GO:0006974), protein transport (GO:0030154), cell differentiation (GO:0015031), and RNA-binding (GO:0003723) pathways (***Figure 5G***). In contrast to WD testes, we observed an integrated gene network based around the expression of *Snrpg* (FC –1.27), *Top1* (FC 1.38), and *Hnrnph1* (FC –1.3) (***Figure 5H***) in MD-WD testes. We also observed networks linked to *H3f3a* (FC –1.14), *Mdm2* (FC 1.24), and *Pcgf2* (FC –1.52) in MD-WD testes. As we identified no differentially expressed genes in LPD (***Figure 5A***) or MD-LPD (***Figure 5B***) testes, we conducted gene ontology analysis of genes displaying a fold change <–1 or >1 and a $p<0.05$. In LPD testes we identified 910 genes (490 downregulated, 420 upregulated) associated with an upregulation of metabolic processes and a downregulation of RNA binding and transcription regulation. In MD-LPD testes, we identified 3425 (2095 downregulated, 1330 upregulated) genes associated with an upregulation of RNA splicing (GO:0008380) and a downregulation of extracellular structure organization (GO:0043062), T cell activation (GO:0046631), and MAPK regulation (GO:0043410).

Paternal low-protein diet alters early placental morphology and metabolism

Recently, we have shown that while our LPD, MD-LPD, WD, and MD-WD diets do not detrimentally affect male fertility, they do have a significant impact on post-fertilisation embryonic development (***Morgan et al., 2021b***). To establish whether sub-optimal paternal diet influenced early placental development, whole conceptus morphology was analysed at embryonic (E) day 8.5. We observed no difference in the mean number of implantation sites between groups (***Figure 6A***). However, morphological assessment of whole embryo implantation sites (***Figure 6B***) revealed a significant reduction of invasion depth in LPD embryos compared to MD-LPD embryos (***Figure 6C***). Furthermore, LPD embryos demonstrated a trend towards a smaller EPC area (***Figure 6D***) and an increased angle of misalignment from the central maternal channel (***Figure 6E***) when compared to CD embryos ($p<0.1$). To explore the impact of paternal diet on early placental dynamics further, individual ectoplacental

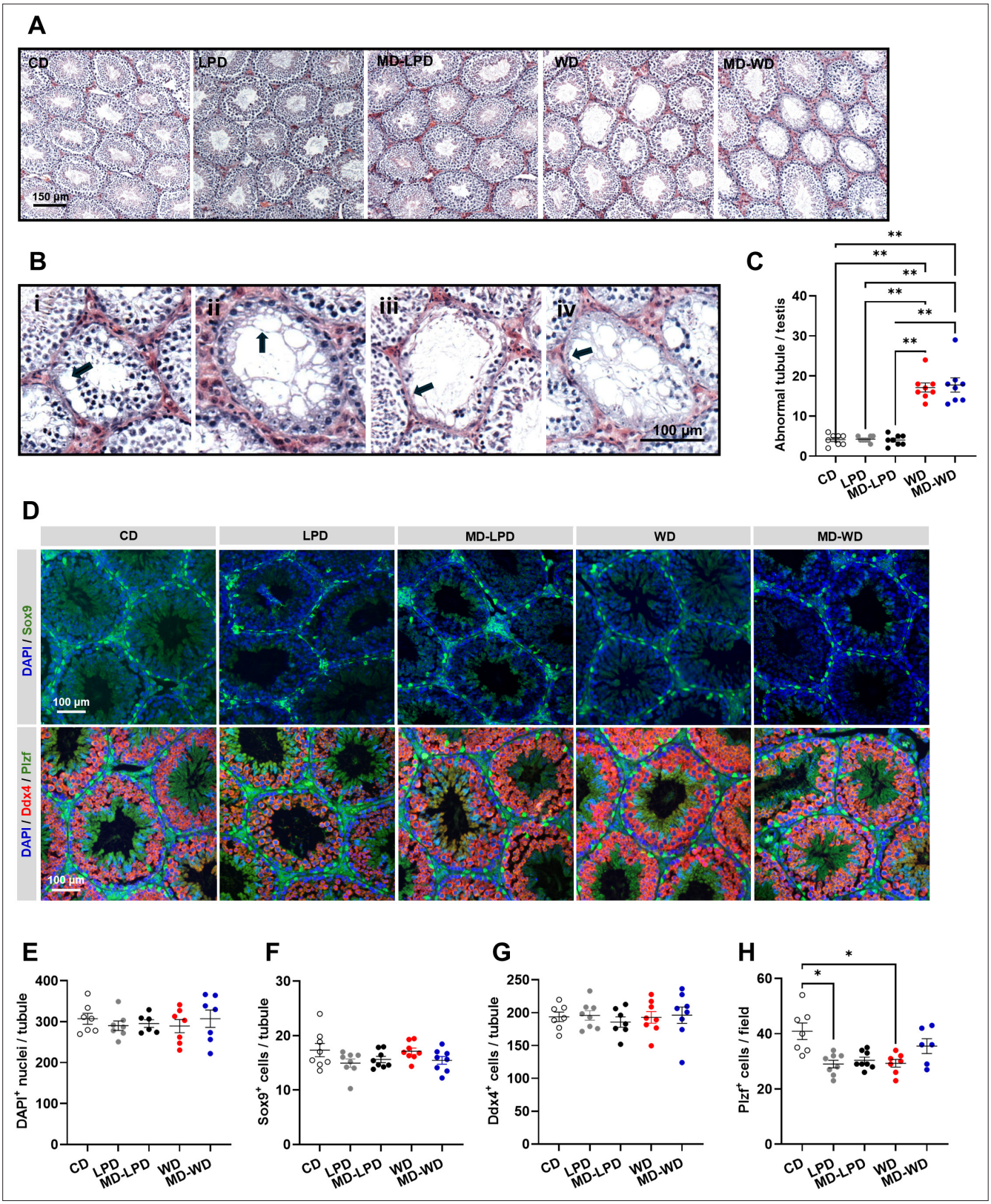

Figure 4. Impact of diet on male testicular morphology. (**A**) Representative images showing tubule morphology in males fed either a control diet (CD), low-protein diet (LPD), methyl donor-supplemented LPD (MD-LPD), Western diet (WD), or methyl donor-supplemented WD (MD-WD). (**B**) Examples of tubule anomalies identified in WD and MD-WD males, including separation of the epithelium from the tubule basement membrane (as indicated by an arrow in i), appearance of vacuoles (as indicated by an arrow in ii), and loss of the germinal epithelium (as indicated by arrows in iii and iv). (**C**) Frequency

Figure 4 continued on next page

Figure 4 continued

of abnormal tubules per testis in males fed either CD, LPD, MD-LPD, WD, or MD-WD. (**D**) Representative staining patterns for DAPI (nuclear counterstain), Sox9 (marker of Sertoli cells), Ddx4 (marker of spermatocytes and spermatids), and Plzf (marker of spermatogonial stem cells) in testes from males fed CD, LPD, MD-LPD, WD, and MD-WD. (**E**) Number of DAPI, (**F**) Sox9, (**G**) Ddx4, and (**H**) Plzf$^+$ cells. *N*=7–8 males in each group. Data are presented as mean ±S EM in C and E–H. Data were analysed using either a one-way ANOVA (panels **E**, **F**, **G**, and **H**) or Kruskal-Wallis test (panel C) with Holm-Sidak or Dunn's post hoc tests for multiple comparison, respectively. *p<0.05, **p<0.01.

The online version of this article includes the following figure supplement(s) for figure 4:

Figure supplement 1. Representative negative control images of testes showing (**A**) no primary antibody controls for Plzf (green) and Dddx4 (red) with DAPI (nuclei) shown in blue.

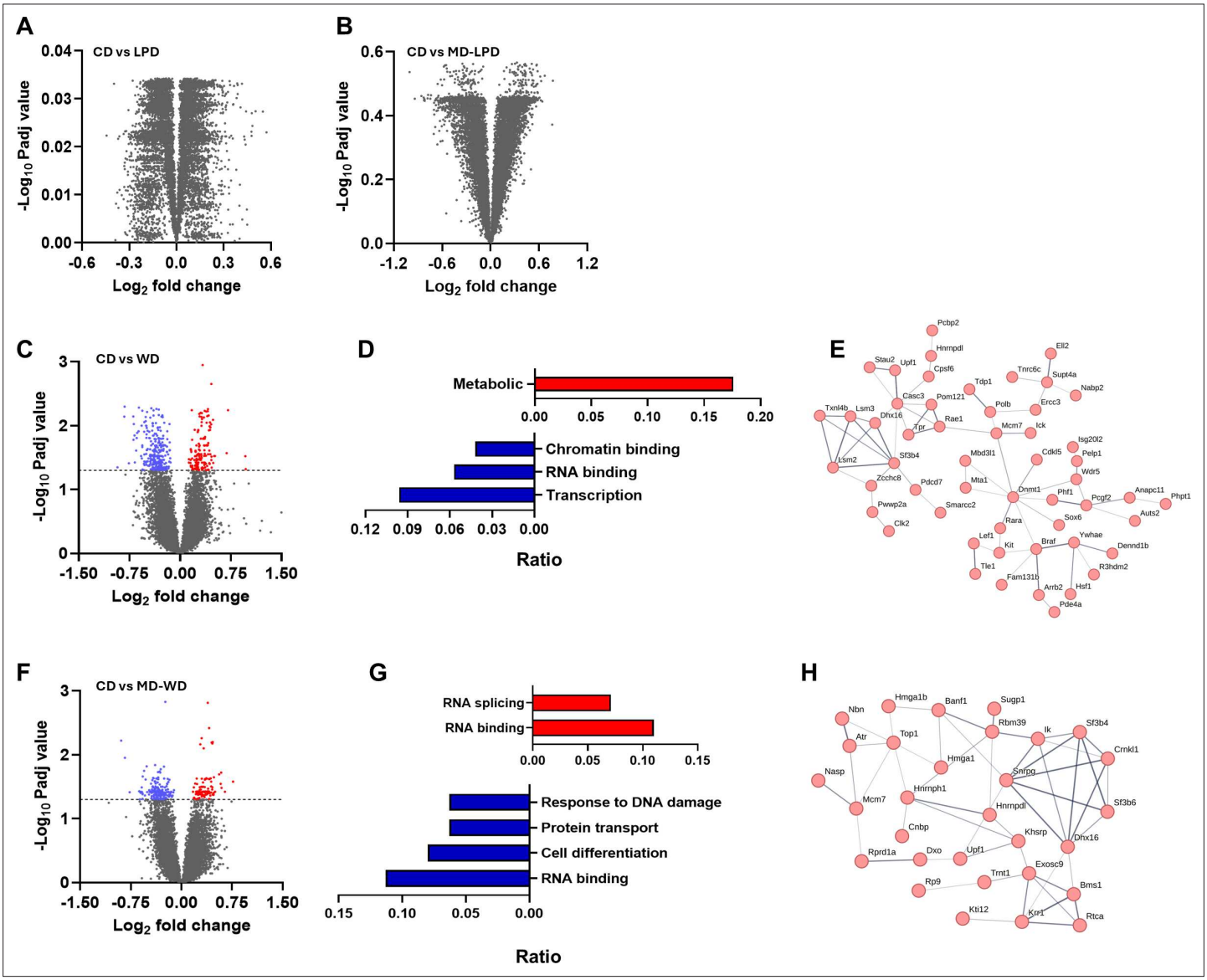

Figure 5. Impact of diet on testicular gene expression. Volcano plots comparing differential gene expression between males fed a control diet (CD) and males fed (**A**) a low-protein diet (LPD), (**B**) methyl donor-supplemented LPD (MD-LPD), or (**C**) Western diet (WD). (**D**) Pathway and (**E**) network analysis of differentially expressed genes between CD- and WD-fed males. (**F**) Volcano plots comparing differential gene expression between males fed a CD and males fed a methyl donor-supplemented WD (MD-WD). (**G**) Pathway and (**H**) network analysis of differentially expressed genes between CD- and MD-WD-fed males. *N*=8 males in each group.

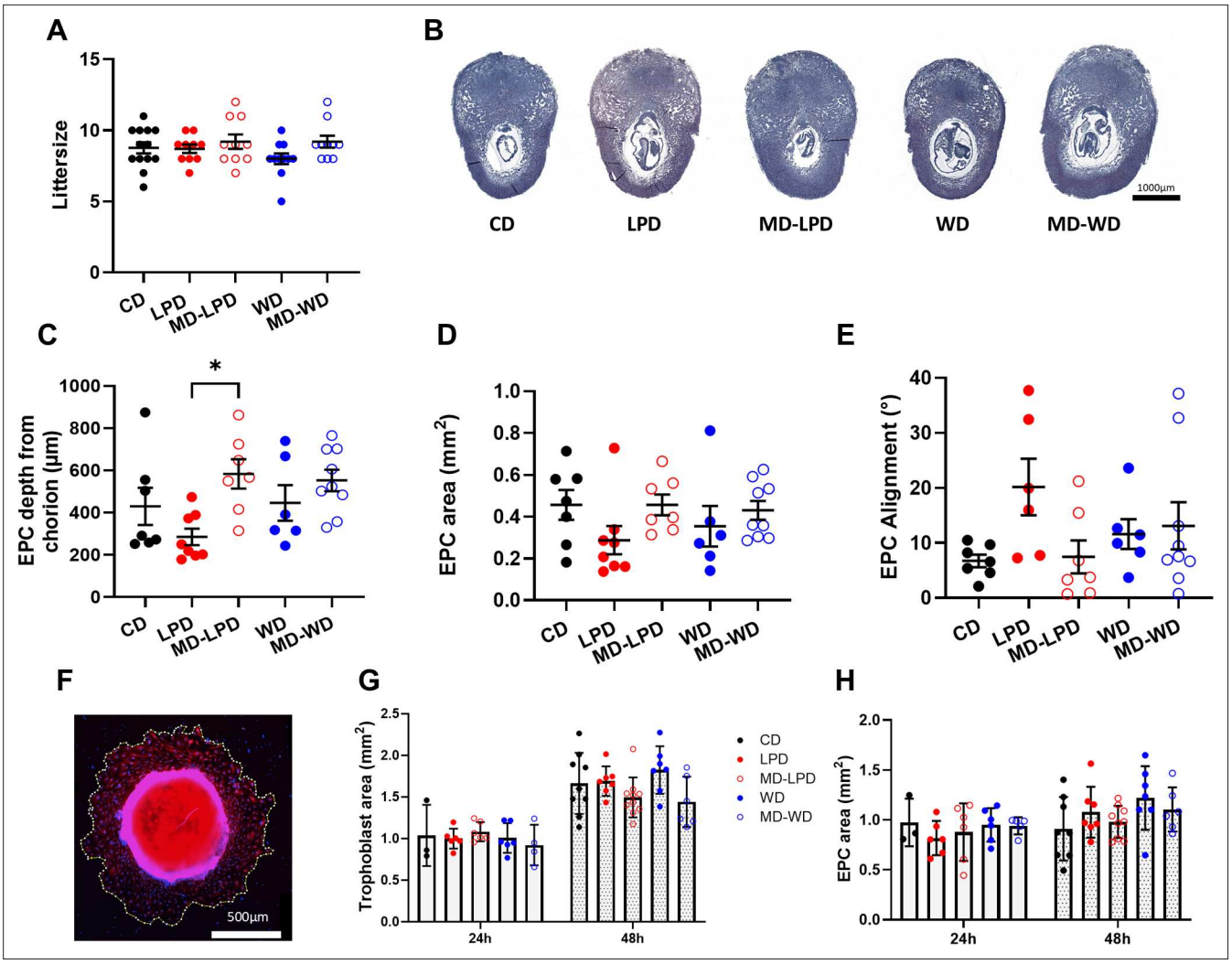

Figure 6. Impact of paternal diet on early (embryonic day [E]8.5) placental development. (**A**) Litter size at E8.5 from males fed either a control diet (CD), low-protein diet (LPD), methyl donor-supplemented LPD (MD-LPD), Western diet (WD), or methyl donor supplemented WD (MD-WD) prior to mating. (**B**) Representative images of haematoxylin and eosin (H&E)-stained whole E8.5 conceptuses. Ectoplacental cone (EPC) (**C**) invasion depth, (**D**) area, and (**I**) alignment. (**F**) Representative EPC outgrowth after 48 hr in culture, stained for α-tubulin. (**G**) Trophoblast and (**H**) EPC area at 24 and 48 hr time points. *N*=10–13 litters in A, derived from a minimum of 8 separate stud males per group, and 4–9 conceptuses in C–H, each from a separate litter and stud male. Data are presented as mean ± SEM in A, C–E and G–H. Data were analysed using either a one-way ANOVA or Kruskal-Wallis test with Holm-Sidak or Dunn's post hoc tests for multiple comparison, respectively. *p<0.05.

cones (EPCs) were isolated and cultured for either 24 or 48 hr (***Figure 6F***). There was no difference in mean trophoblast outgrowth (***Figure 6G***) or central EPC area (***Figure 5H***) in either the 24 or 48 hr explants.

Sup-optimal paternal diet alters fetal weights in late gestation in a sex-specific manner

Next, we examined the impact of paternal diets on late gestation (E17.5) fetal and placental development. There was no difference in mean fetal weight between groups. However, in both LPD and MD-LPD groups, a significantly higher proportion of fetuses displayed a weight below the 10th centile when compared to CD fetuses (15% and 19%, respectively, p<0.05, ***Figure 7A***). No differences in fetal weight distribution were observed in either WD or MD-WD groups (***Figure 7A***). When fetal weights were separated by fetal sex, LPD, MD-LPD, and MD-WD female fetuses were significantly lighter than CD females (p<0.05; ***Figure 7B***). However, there were no differences in mean fetal weight between any of the male groups (***Figure 7C***). When assessing the influence of fetal sex

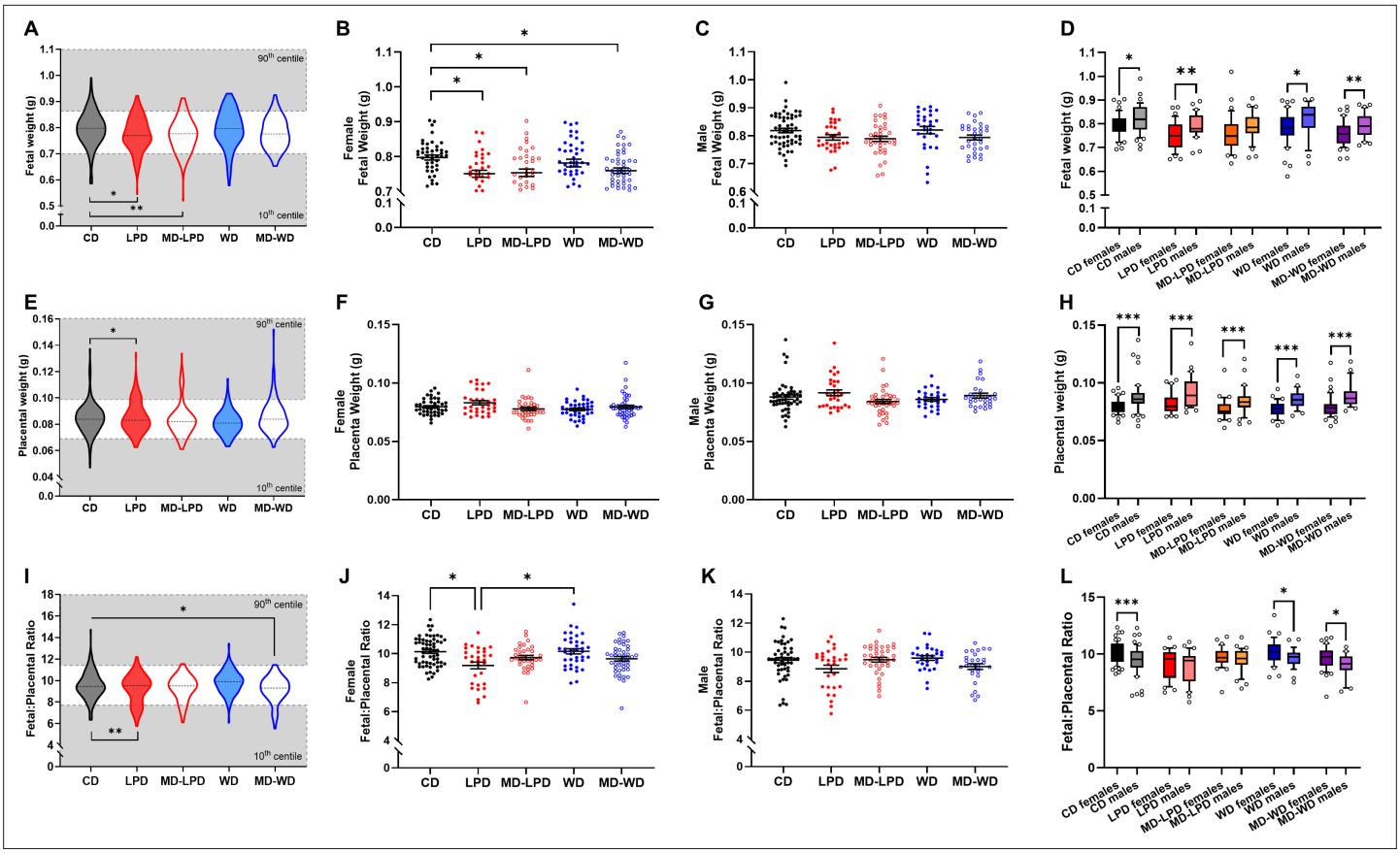

Figure 7. Impact of paternal diet on fetal and placental weight in late (embryonic day [E]17.5) gestation. (**A**) Late gestation fetal weight and distributions above the 90th centile and below the 10th centile of control diet (CD) fetal weights from males fed either a CD, low-protein diet (LPD), methyl donor-supplemented LPD (MD-LPD), Western diet (WD), or methyl donor-supplemented WD (MD-WD) prior to mating. Late gestation (**B**) female, (**C**) male, and (**D**) intra-diet comparison of fetal weight. (**E**) Late gestation placental weight and distributions above the 90th centile and below the 10th centile of CD placental weights. Late gestation (**F**) female, (**G**) male, and (**H**) intra-diet comparison of placental weight. (**I**) Late gestation fetal:placental ratio and distributions above the 90th centile and below the 10th centile of CD fetal:placental ratio. Late gestation (**G**) female, (**H**) male, and (**I**) intra-diet comparison of fetal:placental weight ratio. *N*=10–13 litters, derived from a minimum of 8 separate stud males per group. Data are presented as mean ± SEM or as box plots with the mean and individual data points outside of the 10–90th percentile. Data are presented as mean ± SEM andwere analysed using a generalised linear mixed model analysis with paternal origin of litter and duration on respective diet incorporated as random effects (panels **A**, **B**, **C**, **E**, **F**, **G**, **I**, **J**, and **K**) or t-test (panels **D**, **H**, and **L**) following assessment for normality using a Shapiro-Wilk test. *p<0.05, **p<0.01, ***p<0.001.

on weight, we observed that males were typically heavier than females, with the difference being significant for CD, LPD, WD, and MD-WD males when compared to their respective females (p<0.05, ***Figure 7D***).

Analysis of mean placental weight showed no difference between groups. However, placentas from LPD-fed males showed a higher proportion above the 90th centile for weight when compared to CD males (***Figure 7E***, p<0.05). Analysis of placental weight by fetal sex showed no difference for either females (***Figure 7F***) or males (***Figure 7G***) in any groups. However, in line with fetal weight, males had heavier placentas than females in all groups (p<0.001, ***Figure 7H***).

Finally, while there was no difference in mean fetal:placental ratio across all groups, a significantly higher proportion of LPD fetuses displayed a ratio below the 10th centile, and MD-WD fetuses showed a reduction in the number above the 90th centile (***Figure 7I***; p<0.05), when compared to CD fetuses. Analysis of fetal:placental ratio revealed a significantly lower ratio in LPD females when compared to CD and WD females (p<0.05, ***Figure 7J***). In contrast, no differences between any of the male groups was observed (***Figure 7K***). When comparing females to males, we observed a lower fetal:placental ratio in CD, WD, and MD-WD males (p<0.05, ***Figure 7L***) when compared to their respective females. However, no differences were observed between LPD or MD-LPD males and females (***Figure 7L***).

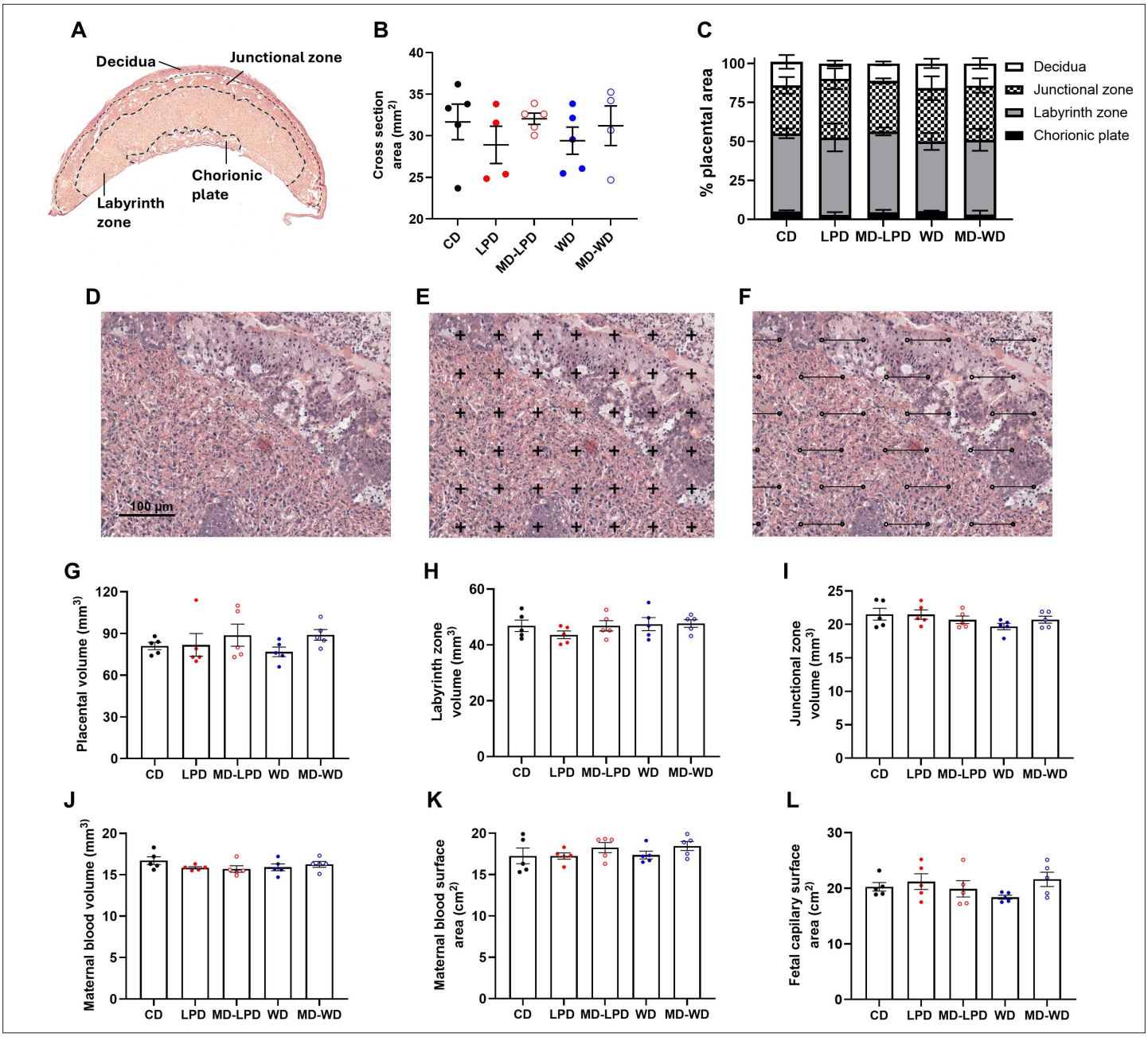

Figure 8. Analysis of late gestation (embryonic day [E]17.5) placental morphology in response to paternal diet. (**A**) Representative image of a cross section through the late gestation (E17.5) placenta highlighting the decidua, junctional zone, labyrinth zone, and chorionic plate regions. (**B**) Cross-sectional area and (**C**) relative regional composition of placentas derived from males fed either a control diet (CD), low-protein diet (LPD), methyl donor-supplemented LPD (MD-LPD), Western diet (WD), or methyl donor supplemented WD (MD-WD) prior to mating. (**D**) Representative images of an E17.5 placenta at ×20 magnification prior to the application of (**E**) estimation of compartment global volumes using Cavalieri's principle with a grid comprising a test system of points and (**F**) stereological method for estimating the surface density of maternal blood vessels and fetal capillaries using a grid comprising isotropic lines. E17.5 placental (**G**) volume, (**H**) labyrinth zone volume, (**I**) junctional zone volume, (**J**) maternal blood space volume, (**K**) maternal blood surface area, and (**L**) fetal capillary surface area. *N*=5 placentas per group, each from separate litters and stud males. Data are presented as mean ± SEM and were analysed using a one-way ANOVA (panels **B**, **G–L**) or Kruskal-Wallis test (panel B) with post hoc correction where appropriate.

Paternal sub-optimal diet has minimal impact on placental morphology

As fetal placental ratio appeared altered in response to paternal diet, we next assessed placental morphology, measuring the relative areas of the decidua, junctional zone, labyrinth zone, and chorionic plate (***Figure 8A***). There was no difference in mean cross-sectional area (***Figure 8B***) or in the relative proportion of each placental compartment (***Figure 8C***) between diets. Additionally, we undertook a stereological analysis of placenta morphology (***Figure 8D–F***) observing no difference in mean placental volume (***Figure 8G***), labyrinth zone volume (***Figure 8H***), junctional zone volume (***Figure 8I***), maternal blood volume (***Figure 8J***), maternal blood surface area (***Figure 8K***), or fetal capillary surface area (***Figure 8L***).

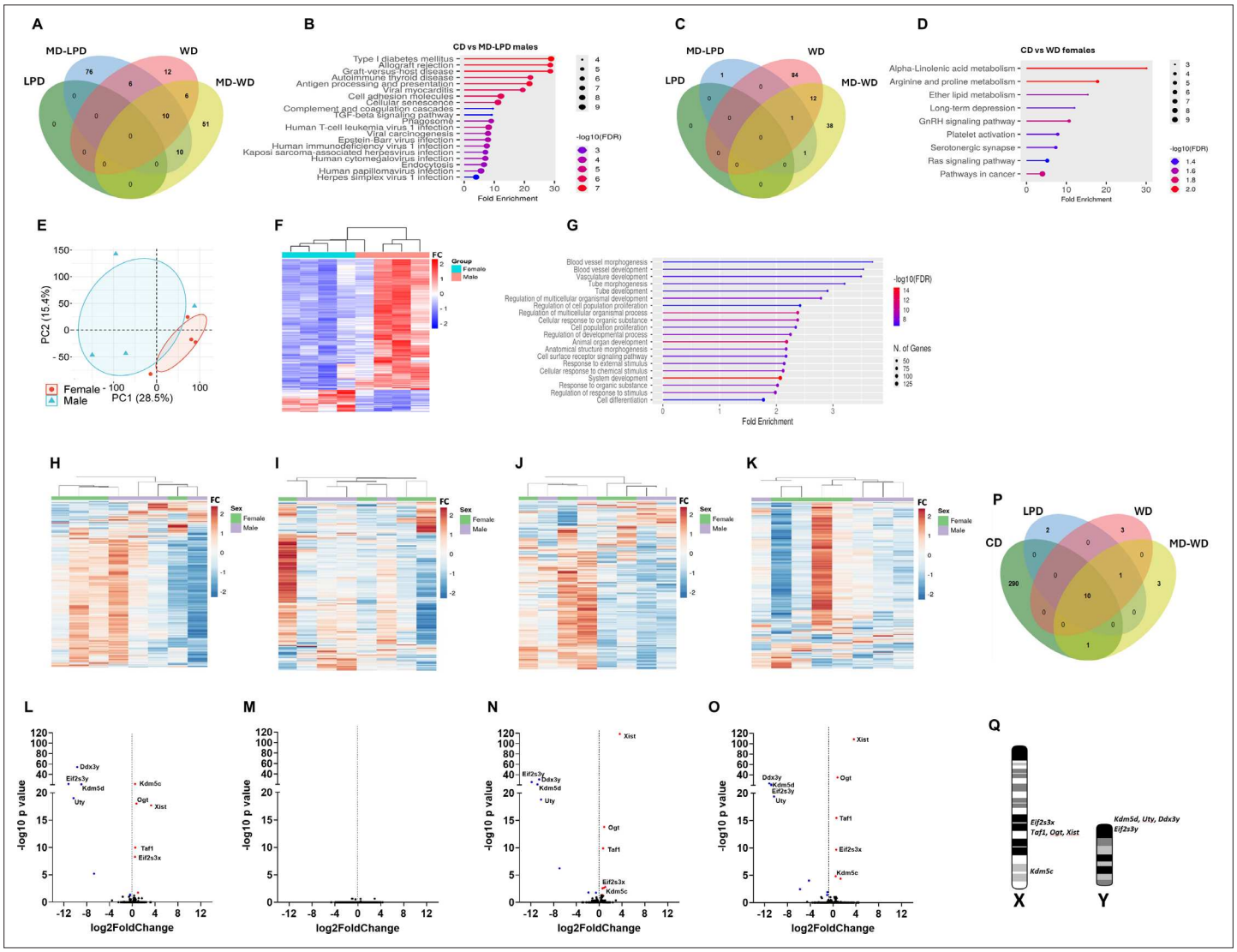

Figure 9. Late gestation (embryonic day [E]17.5) placental gene expression is altered in a diet- and sex-specific manner. (**A**) Differential gene expression and (**B**) pathway analysis from male placentas derived from males fed either a control diet (CD), low-protein diet (LPD), methyl donor-supplemented LPD (MD-LPD), Western diet (WD), or methyl donor supplemented WD (MD-WD) prior to mating. (**C**) Differential gene expression and (**D**) pathway analysis from female placentas. (**E**) Principal component analysis comparing CD male and female placental gene expression profiles. (**F**) Heatmap of the 301 sexually dimorphic genes between male and female CD placentas and (**G**) the pathway analysis. Heatmaps showing the relative level of expression and clustering of the same 301 genes in (**H**) LPD, (**I**) MD-LPD, (**J**) WD, and (**K**) MD-WD male and female placentas. Volcano plots highlighting the significantly (padj<0.05) upregulated (red) and downregulated (blue) differentially expressed genes between male and female (**L**) LPD, (**M**) MD-LPD, (**N**) WD, and (**O**) MD-WD placentas. (**P**) Overlap of sexually dimorphic genes between male and female CD, LPD, WD, and MD-WD placentas. (**Q**) Chromosomal locations of common X and Y chromosome sexually dimorphic genes between CD, LPD, WD, and MD-WD placentas. *N*=4 male and 4 female placentas, each from separate litters and stud males.

Paternal sub-optimal diets influence sex-specific placental transcriptome

Finally, we performed a transcriptomic analysis of the late gestation placenta by RNA-seq using four male and four female placentas from each dietary group. Initial analysis, separating the results by diet and sex, identified 0, 102, 34, and 77 differentially expressed genes (padj<0.05) between LPD, MD-LPD, WD, MD-WD, and CD male placentas, respectively (***Figure 9A***). Pathway analysis of the 102 differentially expressed genes in MD-LPD male placentas identified pathways involved in metabolism (type 1 diabetes mellitus), immune system regulation (antigen processing, complement and coagulation cascades), cellular adhesion, signalling, and senescence (***Figure 9B***). No significant pathway enrichment was found for the differentially expressed genes in WD or MD-WD male placentas when compared to CD males. Similarly, when comparing female placentas, we observed 0, 3, 97, and 52 differentially expressed genes (padj<0.05) when comparing LPD, MD-LPD, WD, and MD-WD with CD placentas, respectively (***Figure 9C***). Pathway analysis of the 97 differentially expressed genes in WD female placentas identified pathways involved in lipid metabolism and signalling (RAS, GnRH) pathways (***Figure 9D***). No significant pathways were identified for either MD-LPD or MD-WD female placenta differentially expressed genes. These data suggest that paternal diet may be influencing placental gene expression in a sex-dependent manner, with more differentially expressed genes observed within the male MD-LPD and MD-WD groups, while the WD and MD-WD females show a greater change in gene expression profiles. Principal component analysis of expression between CD males and females suggested the existence of a sex-specific profile (***Figure 9E***). Additional analysis identified 301 differentially expressed placental genes between CD males and females (padj<0.05, ***Figure 9F***) (see Supplemental Data S1 for full list). Of these 301 genes, 43 were upregulated in males and 258 were upregulated in females. Gene ontology analysis identified pathways involved in vascular development, developmental processes, and signal transduction (***Figure 9G***). Interestingly, comparison of these same 301 genes in LPD, MD-LPD, WD, and MD-WD placentas showed no such sexual dimorphism (***Figure 9H–K***). In total, we identified 13, 0, 14, and 15 genes to be differentially expressed between males and females in the LPD, MD-LPD, WD, and MD-WD groups, respectively (***Figure 9L–O***). In total, we identified just nine differentially expressed genes, and one unprocessed pseudogene, present in all five dietary groups (***Figure 9P***). Of the nine conserved differentially expressed mRNAs, five were located on the X chromosome (*Eif2s3x, Taf1, Otg, Xist, Kdm5c*), while four were on the Y chromosome (*Kdm5d, Uty, Ddx3y, Eif2s3y*) (***Figure 9Q***). In contrast, LPD placentas displayed sexually dimorphic gene expression on chromosomes 5 and 13, WD placentas had sexually dimorphic gene expression on chromosomes 3, 5, and 15, and MD-WD demonstrated sexually dimorphic gene expression on chromosomes 3, 5, 6, and 14 (see Supplementary Data S1).

Discussion

Consumption of an unbalanced or unhealthy diet is a major risk factor for a range of diseases such as obesity, diabetes, and cardiovascular disease. Poor parental diet prior to conception also impacts on patterns of post-fertilisation development, shaping fetal and placental dynamics, and increases the risk for a range of non-communicable disorders in adult life (***Ozanne et al., 2004***). Under the current study, we explored the impact of both paternal under- (LPD) and over-nutrition (WD) on male reproductive health, fetal growth, and placental development. We also investigated the impact of supplementing these diets with a range of methyl donors and carriers to define if their use could negate any detrimental influences imposed by the diets. We observed that males consuming a high-fat/sugar diet (WD and MD-WD) displayed a series of physiological changes in their metabolic health, gut bacterial profiles, and testicular morphology and gene expression. While both over- and under-nutritional regimens had no impact on fundamental male fertility, we observed significant changes in fetal and placental weights in late gestation. Furthermore, we observed a significant loss in sexual dimorphism in the late gestation placenta. While sex-specific differences in fetal and adult offspring are reported widely in response to both maternal and paternal diet (***Dearden et al., 2018***; ***Rosenfeld, 2015***), our data provide additional insight into how sex-specific paternal programming may be mediated during development.

While we observed minimal impact of the LPD and MD-LPD on male metabolic health, mice fed the WD and MD-WD displayed significant changes in adiposity and hepatic cholesterol and FFAs.

Excessive accumulation of cholesterol and FFAs within the liver are central hallmarks of metabolic conditions, such as NAFLD and MASLD. While elevated hepatic FFAs have been linked to insulin resistance and elevated levels of proinflammatory mediators, we observed no change in circulating glucose, insulin, or Tnf levels. This is in line with studies showing that nearly half of patients with NAFLD/MASLD also do not present with insulin resistance (**Singh et al., 2015**), highlighting its heterogenous nature. Changes in metabolic status have also been linked to gut dysbiosis. We observed differences in the abundance of Defferibacteres, Proteobacteria, and TM7 in fecal samples from WD and MD-WD males. Similar increases in Deferribacteres have been observed in mice maintained on high-fat diets (**Liu et al., 2019**; **Serino et al., 2012**), while the abundance of TM7 has been linked with elevated BMI, fat mass, and inflammatory status in humans (**Gomes et al., 2020**). Separately, negative links between TM7 abundance and body weight and adiposity in rodents have been identified (**de la Garza et al., 2022**; **Hu et al., 2022**). While our study indicates significant shifts in male metabolic homeostasis, further studies are needed to define how metabolic, inflammatory, and microbiota status interact and their impact on male reproductive health. For example, bacterial metabolites such as 5-hydroxytryptamine have been shown to promote sperm hyperactivation and the acrosome reaction in mice (**Sugiyama et al., 2019**), hamsters (**Fujinoki, 2011**), and men (**Omote et al., 2023**). Additionally, many polyunsaturated fatty acids produced by the gut microbiota have a significant role in stabilising the sperm plasma membrane (**Lv et al., 2024**). Finally, additional microbiota-derived metabolites such as androgens (**Colldén et al., 2019**) and hormones, including GLP-1 and peptide YY (PYY) (**Cannarella et al., 2021**), have been associated with changes in sperm production. Interestingly, studies have also shown that fecal transplants can be used to treat infertility and improve sperm quality in mice (**Hao et al., 2022**; **Zhang et al., 2021**). Therefore, additional studies, with the inclusion of a methyl donor CD (MD-CD), are required to better understand the connections between dietary-induced gut dysbiosis and male reproductive fitness.

Within the testis, LPD and WD males displayed a significant reduction in the number of undifferentiated spermatogonial stem (Plzf+) cells when compared to CD males, while no difference was observed in MD-LPD and MD-WD males. While the loss of Plzf is not detrimental for spermatogenesis, Plzf ensures spermatogonial stem remain in a state of undifferentiation, interacting with other transcription factors such as SRY-box TF 3 (SOX3) and Spalt-like TF 4 (SALL4) to establish the chromatin and transcription landscape in spermatogonial stem cells (**Yi et al., 2025**). However, the regulation of Plzf by methyl donors is currently undetermined. Separately, WD and MD-WD males displayed an increased rate of tubule abnormalities when compared to CD males. In rodents, exposure to a high-fat diet has been shown to induce tubule vacuolization atrophy (**Ghosh and Mukherjee, 2018**), as well as disrupting the essential adhesion between spermatogenic and Sertoli cells, resulting in Sertoli cell atrophy (**Liu et al., 2014**). Sertoli cells are essential for supporting spermatogenesis and their loss is associated with male infertility. Sertoli cells also produce inhibin β and its serum levels correlate positively with testicular size and sperm production rates (**Luisi et al., 2005**). Inhibin production is also tightly linked to the secretion of FSH from the pituitary, providing a negative feedback signal to regulate spermatogenesis. As we observed a significant elevation in serum inhibin β-A in WD males, but no change in Sertoli ($Sox9^{+}$) cell number or fundamental male fertility, the increase in inhibin β might indicate a dysfunction in normal hypothalamic-pituitary-testis axis regulation. However, further studies are needed to confirm this.

Analysis of testicular gene expression revealed minimal changes in response to LPD or MD-LPD. In contrast, testes from WD- and MD-WD-fed males displayed an upregulation of genes involved in fatty acid metabolism, mRNA processing, Wnt signalling, and protein transport processes, and a downregulation of transcription-related genes. The increase in genes associated with fatty acid metabolism (*Acadsb*, *Crat, Pla2g5*, *Daglb, Mgll*) and glycolytic components (*Pdha1, Hk2*) link with the changes observed in metabolic status in these males. Furthermore, we observed upregulation of *Paf1* and *Ctr9*, both components of the Paf1C complex. PAF1C associates with the promoter and coding sequences of active genes (**Pokholok et al., 2002**) and interacts with a series of transcriptional elongation factors (**Pokholok et al., 2002**; **Squazzo et al., 2002**). Studies have identified Paf1C as crucial for the acquisition of transcription-associated histone modifications, such as H3 methylation at K4, K36, and K79 (**Cao et al., 2015**; **Mbogning et al., 2013**). Interestingly, we identified an increase in the expression of the histone variants *H3f3a* and *H3f3b*. Unlike most other canonical histones, H3.3 is not completely removed from the chromatin during spermatogenesis

and is enriched at genomic regions important for zygotic development in mice and men (**Brykczynska et al., 2010**; **Hammoud et al., 2011**). Studies have shown that disruption of H3K4me2 marks in mouse sperm have significant consequences for offspring health over multiple generations (**Siklenka et al., 2015**), and levels of sperm H3K4me2 may serve as a metabolic sensor linking paternal diet with offspring metabolic ill-health predisposition (**Pepin et al., 2022**). The downregulation of transcription-regulating genes, such as *Dnmt1, Mta1, Phf1, Pwwp2a, Wdr5, Hsf1, Nfrkb, Pelp1, Prox1,* and *Rara,* suggests that paternal HFD might influence differential patterns of testicular transcriptional regulation, which could affect sperm composition and post-fertilisation development (**Cui et al., 2025**). Finally, we observed a downregulation of multiple RNA-binding genes in both WD and MD-WD testes. Recently, the significance of RNA-binding proteins as critical regulators of spermatogenesis and sperm function has been recognised (**Li et al., 2024**). As many RNA-binding proteins play central roles in orchestrating intricate transcriptional and post-transcriptional regulatory networks, their function as essential regulators of testicular germ cell development is becoming defined (**Gao et al., 2026**).

Together, these findings suggest that sub-optimal male diets have the potential to alter sperm modifications, which are not simply corrected by methyl donor supplementation. To determine whether these paternal diet-driven changes to male reproductive physiology impacted on post-fertilisation dynamics, we analysed early (E8.5) and late (E17.5) fetal and placental development. Analysis of E8.5 placental invasion revealed that poor paternal diet had minimal impact on overall morphology or invasion depth in vivo. However, we observed significant sex-specific influences of paternal diet on late gestation fetal and placental growth. During fetal development, differences in patterns of male and female growth have been described from as early as the first trimester with males growing at a faster rate (**Broere-Brown et al., 2016**). We identified over 300 sexually dimorphic, differentially expressed genes between CD males and females, with the majority being upregulated in females. Gene ontology analysis identified vascular, immunological, extracellular matrix organisation, and cell-signalling pathways as being differentially expressed, mirroring observations from male and female term placentas in humans (**Buckberry et al., 2014**). While female human term placentas have increased expression of multiple immune regulation genes when compared to males (**Sood et al., 2006**), Y-chromosome genes, such as *Ddx3y*, *Uty*, and *Kdm5d*, encode epitopes that contribute to minor histocompatibility antigens present throughout the placenta (**Cvitic et al., 2013**). Studies have also shown that cultured trophoblast tissues isolated from human healthy male placentas secrete more TNF and less IL-10 in response to lipopolysaccharide than female tissues (**Yang et al., 2021**). In contrast, genes such as *Tgfb1*, which was upregulated in CD females, are critical in regulating fetal-maternal immune tolerance (**Yang et al., 2021**). Furthermore, studies have shown female placentas to be more responsive to shifts in maternal inflammation and dietary status than males (**Osei-Kumah et al., 2011**; **Sedlmeier et al., 2014**). Similar to our data, studies have also reported upregulation of receptor-ligand signalling in human female placentas, including several collagens, laminins, and integrins, suggestive of an enhanced invasion and placentation potential (**Braun et al., 2021**). Finally, we observed upregulation of genes involved in steroid synthesis and endocrine regulation in female placentas. Placental endocrine function operates to regulate both maternal physiological response and fetal development (**Stern et al., 2021**). In contrast to our CD males and females, all other groups displayed a dramatic loss of sexual dimorphism. While the underlying mechanism(s) for our observed loss of sexual dimorphism are unknown, perturbed paternal sperm epigenetic status could modulate early embryo X-chromosome inactivation and/or X-chromosome dosage in females, resulting in differential profiles of autosomal gene expression (**Gonzalez et al., 2018**; **Petropoulos et al., 2016**).

Collectively, we observe that paternal LPD or WD, with or without supplementation, had no impact on overall male fertility, but have influences on male reproductive physiology. While paternal LPD induced minor changes in early placental morphology and metabolism, these effects were small, and the consequences of these changes remain to be defined. In late gestation, paternal diet affected fetal development in a sex- and diet-specific manner. While we observed significant sexual dimorphism in gene expression patterns between CD males and females, these differences were largely removed in response to our experimental diets. Such loss of sexual dimorphism could provide one process through which poor paternal diet programmes offspring ill-health in adulthood. However, the precise mechanisms through which this occurs remain to be determined.

Materials and methods

Mice diet regime and matings

All animal procedures were conducted in accordance with the UK Home Office Animals (Scientific Procedures) Act 1986 and carried out under Project License PP8899264 with local ethical approval at University of Nottingham. C57BL/6J mice (Charles River, UK) were housed in controlled 12/12 hr light/dark conditions with a constant temperature (21°C±3°C) and ad libitum access to water. Virgin 8-week-old males (*n*=8 per treatment group) were fed either CD (18% casein, 21% sucrose, 0% milk fat, 0% cholesterol), isocaloric LPD (9% casein, 24% sucrose, 0% milk fat, 0% cholesterol), WD (19% casein, 34% sucrose, 20% milk fat, 0.15% cholesterol), or LPD or WD supplemented with methyl donors and carriers (5 g/kg diet choline chloride, 15 g/kg diet betaine, 7.5 g/kg diet methionine, 15 mg/kg diet folic acid, 1.5 mg/kg diet vitamin B12; termed MD-LPD or MD-WD, respectively) for up to 24 weeks. Exact dietary formulations are outlined in ***Supplementary file 1***. Virgin female C57BL/6J mice were maintained on standard rodent chow (rat/mouse No.1 maintenance diet, Special Diet Services) throughout the study. Females were mated at 9 weeks of age (±7 days) with stud males who had been fed their respective diet for a minimum of 8 weeks. Successful mating was confirmed by the presence of a copulation plug and denoted as embryonic day (E)0.5. Dams were euthanized via cervical dislocation on either E8.5 for the collection of EPCs or E17.5 for fetal and placental tissues. Stud males were culled by cervical dislocation for the collection and storage of tissues. Blood was collected via heart puncture, allowed to clot on ice and centrifuged at 10,000×*g*, 4°C for 10 min before storage of the serum at −80°C. Heart, kidney, liver, testis, and caudal epididymis were dissected, weighed, and either snap-frozen prior to storage at −80°C or fixed overnight in 10% neutral buffered formalin (Sigma, UK) at 4°C before processing and embedding in paraffin wax. Fecal pellets were collected from the descending colon using sterile forceps and placed in 2 ml DNase/RNase-free collection tubes, snap-frozen, and stored at –80°C. A second batch of males (*n*=6) were fed using the same experimental protocol and utilised for the analysis of fat pad mass.

Stud male metabolic status assessment

Stud male non-fasting serum glucose was measured using the Glucose Colorimetric Detection Kit (EIAGLUC, Thermo Fisher Scientific, UK), non-fasting insulin was measured using a Rat/Mouse Insulin ELISA Kit (EZRMI-13K; Millipore, UK), Tnf was measured using the TNF alpha SimpleStep ELISA Kit (ab208348, Abcam), inhibin β-A chain was measured using the FineTest Mouse Inhba ELISA Kit (EM0273, Wuhan Fine Biotech Co., China), non-fasting liver tissue total cholesterol was measured using the Cholesterol Quantification Kit (MAK043, Sigma-Aldrich, UK), non-fasting hepatic FFAs were measured using the Free Fatty Acid Quantitation Kit (MAK044, Sigma-Aldrich, UK), and non-fasting hepatic triglycerides were measured using the Triglyceride Quantification Kit (MAK266, Sigma-Aldrich, UK), all in accordance with the manufacturer's instructions.

Gut microbiota sequencing

DNA was extracted from stool pellets using the QIAamp DNA Stool Mini Kit (QIAGEN, UK) following the manufacturer's instructions and stored at –80°C. 16S rDNA sequencing (V3-V4 region) was conducted as described previously (***Batra et al., 2022***). The extracted stool DNA samples (*n*=6 per diet group) were sequenced using the Illumina MiSeq Reagent kit v3 on the Illumina MiSeq platform (Illumina), in accordance with Illumina 16S Metagenomic Sequencing Library Preparation protocol. Briefly, 16S rRNA amplicons were generated using the forward 5' (TCGTCGGCAGCGTCAGATGT GTATAAGAGACAGCCTACGGGNGGCWGCAG) and reverse 5' (GTCTCGTGGGCTCGGAGATG TGTATAAGAGACAGGACTACHVGGGTATCTAATCC) primers, flanked by Illumina adapter-overhang sequences. Illumina dual index barcodes (Illumina XT Index Kit v2, Set A: FC-131-2001) were attached to each amplicon. PCR clean-up was conducted using AMpure XP beads (Beckman; A63882). Library fragment-length distributions were analysed using the Agilent TapeStation 4200 and the Agilent D1000 ScreenTape Assay (Agilent; 5067–5582 and 5067–5583). The generated libraries were pooled in equimolar amounts and the pool was size selected using the Blue Pippin (Sage Science) and a 1.5% Pippin Gel Cassette (Sage Science; BDF2010). The samples were then run over a shared 300 paired end (PE) MiSeq run to deliver about 60–80,000 PE reads per sample. The sequencing run additionally had a 20% PhiX library spike-in as an internal quality control. Raw reads were processed by Qiime2 pipeline and trimmed. Greengenes version 13.8 was used in the classification (***Caporaso et al., 2010***).

Testicular histology

Paraffin-embedded testis tissue (*n*=8 per group) was sectioned at 5 µm using a Leitz 1512 rotary microtome (Leica). For analysis of seminiferous tubule morphology, sections were processed and stained with haematoxylin-eosin (H&E) prior to imaging using a Leica DMRB microscope with an Oasis glide scanner. Image analysis was carried out using Fiji. For each testis sample, an average of 50 seminiferous tubule cross sections were analysed.

For the determination of seminiferous tubule cell types, additional testis sections were dewaxed, rehydrated into PBS, and equilibrated in 100 mM citrate buffer (pH 6.0) at room temperature (RT) prior to being microwaved in 0.1 M tri-sodium citrate buffer (pH 6.0) for 5 min. The sections were incubated in blocking solution (5% bovine serum albumin, 20% normal goat serum in 0.1% Triton X-100 in PBS; Sigma, UK) for 1 hr before incubating with anti-Ddx4 antibody (to identify germ cells; ab27591, 1:100; Abcam, UK) or rabbit anti-Sox9 antibody (to identify Sertoli cells: ab5535, 1:500; Chemicon, UK) in blocking solution, and incubated at 4°C overnight. Slides were washed (three times in 0.1% Triton X-100 in PBS; PBST) prior to incubation in Alexa Fluor 568 (A-21124, 1:200; Invitrogen, UK) in blocking solution for the detection of Ddx4. For the detection of Sox9, slides were incubated with goat anti-rabbit biotinylated antibody (E0432, 1:200; DakoCytomation, UK) for 1 hr in the dark in blocking solution prior to Alexa Fluor 488 streptavidin conjugate, washed in PBST prior to incubation with Alexa Fluor 488 (S-32354, 1:200; Invitrogen, UK) in blocking solution for 30 min at RT. For the detection of Plzf, sections were incubated overnight with anti-Plzf antibody (to identify spermatogonial stem cells: ab189849, 1:3000; Abcam, UK) at 4°C. Sections were washed in PBST prior to incubation with Alexa Fluor 568 (ab175471, 1:200; Abcam) in blocking solution for 1 hr at RT. Negative controls (absence of primary or secondary antibodies) were also conducted to confirm staining specificity (see ***Figure 4—figure supplement 1***). Slides were washed (PBST) before mounting with Antifade Mounting Media with DAPI (Vectashield, UK). Sections were imaged using a Nikon Eclipse 90i fluorescent microscope with a mercury-fibre illuminator Nikon Intensilight C-HGFI and a Hamamatsu ORCA-ER Digital camera (C4742-80) at ×10 and ×20 magnification. Images were analysed using Volocity (Quorum Technologies Inc) with an average of 50 seminiferous tubules counted per male.

Testicular micro-array

Total RNA was extracted from frozen testicular tissues using the RNeasy Plus Mini Kit (QIAGEN; UK) following the manufacturer's instructions. Testicular RNA was diluted to 100 ng/µl using RNAse-free water (QIAGEN, UK) prior to RNA integrity assessment on a Bioanalyzer 2100 platform (Agilent, UK). Samples with an RIN >7 were used for analysis. The GeneChip WT PLUS Reagent Kit (Thermo Fisher Scientific, UK) was used to prepare RNA samples for whole transcriptome expression analysis with GeneChip Whole Transcript (WT) Expression Arrays, as per the manufacturer's instructions. First-strand cDNA was synthesised from the extracted RNA using Reverse Transcriptase, followed by a second-strand cDNA (ss-cDNA) synthesis using DNA Polymerase and RNAse H. Complementary RNA (cRNA) was synthesised by in vitro transcription of the ss-cDNA using T7 RNA polymerase and purified. The purified ss-cDNA was enzymatically fragmented and labelled by terminal deoxynucleotidyl transferase (TdT) using the provided DNA Labelling Reagent following the manufacturer's instructions prior to hybridisation onto the Clariom S Assay Mouse GeneChip (Thermo Fisher Scientific, UK). Data analysis was performed using the Partek Genomics Suite 6.6 analysis software. Comparative analysis between the five diet groups was performed using standard one-way ANOVAs. Dysregulated transcripts were classified based on false discovery rate (FDR)=0.05, fold change <±1.1, and $p \leq 0.05$. The functional annotation and enrichment analysis web tool WEB-based GEneSeTAnaLysis Toolkit (WebGestalt) (***Liao et al., 2019***) was used for gene set enrichment analysis. Network analysis was conducted using Network Analyst (https://www.networkanalyst.ca/NetworkAnalyst/home.xhtml). All gene expression data is publicly available via Gene Expression Omnibus (GSE279868).

In vivo EPC invasion

Formalin-fixed, paraffin-embedded E8.5 whole implantation sites were sectioned to the mid-point as indicated by appearance of the maternal channel. H&E staining was conducted on 5 µm sections and whole sites were imaged at ×20 magnification using a Leica DMRB microscope with an Oasis glide scanner. Images were imported into Fiji for the assessment of total EPC, trophoblast specific area, depth of invasion (measured from chorion to the furthest trophoblast going in the direction of the

maternal channel), and alignment of invasion measured according to ***Wilkinson et al., 2021***, within the implant site and was conducted by a blinded observer.

Isolation and culture of EPC explants

The isolation and culture of E8.5 EPCs was conducted as previously described (***Watkins et al., 2015***). Twenty-four hours prior to dissection, sterile coverslips were coated with BD Matrigel basement membrane matrix (BD Biosciences, Oxford, UK) diluted to 6 mg/ml in RPMI 1640 medium (Life Technologies, UK) and kept at 4°C in four-well plates. On the morning of EPC isolation, the Matrigel-RPMI medium was replaced with 500 µl sterile-filtered RPMI-1640 medium containing 2% KnockOut Serum Replacement (Life Technologies, UK), penicillin-streptomycin-glutamine mix (Life Technologies, UK) and 26.2 µmol 2-mercaptoethanol (Sigma-Aldrich, UK) and allowed to equilibrate at 37°C in 5% CO_2 for at least 1 hr. Whole uteri were excised and placed in pre-warmed (37°C) DMEM (Fisher Scientific, UK) supplemented with 10% (vol/vol) fetal calf serum (Life Technologies, UK). Individual implantation sites were dissected from the uterine tissue and placed in RPMI-1640 medium supplemented with 2% KO-serum replacement (Fisher Scientific, UK), 1% penicillin-streptomycin-glutamine mix (Fisher Scientific, UK) and 26.2 µmol 2-mercaptoethanol (Sigma-Aldrich, UK). The EPCs were then isolated from the decidual capsules and separated from the embryo. The isolated EPCs were then placed onto the Matrigel-coated coverslips and cultured individually at 37°C, 5% CO_2 for either 24 or 48 hr, with a 50% medium change after 24 hr.

After 24 or 48 hr in culture, EPC outgrowths were fixed in 4% neutral buffered formalin (Sigma-Aldrich, UK) for 15 min at RT, washed (1× PBS) and stored at 4°C in PBS. Fixed EPCs were permeabilised with 0.1% Triton X-100 (Sigma-Aldrich, UK) and autofluorescence quenched with ammonium chloride (2.6 mg/ml in PBS; Sigma-Aldrich, UK). Non-specific binding was blocked with 2% BSA in PBS containing 0.1% Triton X-100 for 30 min at RT before overnight incubation at 4°C with a primary antibody for α-tubulin (1:2000; Cell Signaling, Danvers, MA, USA) in PBS with 1% BSA and 0.1% Triton X-100. Following washing (PBS, 0.1% Triton X-100), outgrowths were incubated with the appropriate Alexa Fluor-conjugated secondary antibody (1:10,000; Molecular Probes, Life Technologies, Paisley, UK) for 1 hr at RT and counterstained with DAPI (Sigma-Aldrich, UK) for 10 min before mounting on slides in DPX (Fisher Scientific, Loughborough, UK). All outgrowths were imaged using a Nikon Eclipse 90i fluorescent microscope fitted with a mercury-fibre illuminator, Nikon Intensilight C-HGFI, and a Hamamatsu ORCA-ER Digital camera (C4742-80) and analysed using the Volocity Software. The central EPC was defined as the central, single mass within which individual cell nuclei could not be distinguished from those neighbouring them. Proliferative trophoblast nuclei were defined as those located within the proximity of the central EPC as described previously (***Watkins et al., 2015***).

Placental stereology

At E17.5, dams were culled for the collection of placental tissues. Fetuses and placentas were weighed prior to fixation in Karnovsky's fixative (2.5% glutaraldehyde, 2% formaldehyde in 0.1 M sodium phosphate buffer) for 16 hr at 4°C. Fixed placentas were weighed (wet weight, g) and converted into pre-embedding placental volumes $\left(V_{\text{pre}}\right)$ by dividing wet weight by tissue density (1.05 g/cm^3) prior to multistage systematic and uniformly random sampling (SURS) (***Veras et al., 2008***). Briefly, placentas were cut into approximately six 2 mm slices perpendicular to the chorionic plate. Slices were randomised to generate isotropic uniformly random orientation and embedded in paraffin for stereological estimation of placental compartment volumes, maternal blood volume and surface area, and fetal capillary surface area. Shrinkage correction was performed for each placenta. Shrinkage introduced during dehydration/clearing and paraffin embedding was quantified for each placenta individually by estimating the post-embedding placental volume $\left(V_{\text{post}}\right)$ using the Cavalieri principle (***Howard et al., 2005***; ***Ribeiro et al., 2008***). Each paraffin-embedded 2 mm slice was serially sectioned at 5 µm, and ~10 evenly spaced sections per slice were selected systematically and uniformly random through the block, mounted, and stained with H&E. A point grid was applied to the sampled sections to estimate V_{post} by Cavalieri. The volume shrinkage coefficient for each placenta was calculated as:

$$k_V = \frac{V_{\text{post}}}{V_{\text{pre}}}$$

(with fractional shrinkage $= 1 - k_V$). Absolute compartment volumes estimated from paraffin sections were corrected back to pre-embedding dimensions as:

$$V_{corrected} = \frac{V_{\text{estimated}}}{k_V}$$

Surface area was estimated as the product of surface density and the corresponding shrinkage-corrected placenta volume:

$$S = S_v \times V_{\text{corrected}}$$

where S_v is the surface density estimated by intersection counting and $V_{\text{corrected}}$ is the placenta volume corrected after the paraffin-embedding shrinkage.

Placental RNA extraction and sequencing

Placental RNA was extracted from one quarter of an intact frozen placenta using the miRNeasy Mini Kit (QIAGEN, UK), following tissue disruption in Qiazol (QIAGEN, UK) using the QIAGEN TissueLyserII (25 Hz, 4×30 s), according to the manufacturer's instructions. RNA concentrations were assessed using NanoDrop, and integrity was examined using Agilent 4200 TapeStation and the RNA ScreenTape Assay (Agilent; 5067–5576 and 5067–5577) with an acceptable RIN>8. Stranded RNA-seq libraries were prepared from 1000 ng of total RNA per sample, using the NEBNext Ultra II Directional RNA Library Preparation Kit for Illumina (NEB; E7760) and NEBNext Multiplex Oligos for Illumina (96 Unique Dual Index Pairs) (NEBNext; E6440). Prior to library preparation, total RNA was treated with QIAseq FastSelect -rRNA HMR, to prevent any rRNA present from being converted into sequencing library. Libraries were quantified using the Qubit Fluorometer and the Qubit dsDNA HS Kit (Thermo Fisher Scientific; Q32854). Library fragment-length distributions were analysed using the Agilent 4200 TapeStation and the Agilent High Sensitivity D1000 ScreenTape Assay (Agilent; 5067–5584 and 5067–5585). Libraries were pooled in equimolar amounts and final library quantification was performed using the KAPA Library Quantification Kit for Illumina (Roche; KK4824). The library pool was sequenced on the Illumina NextSeq500 over three NextSeq500 High Output 150 cycle kits (Illumina; 20024907), to generate over 40 million pairs of 75 bp paired-end reads per sample. Raw reads were trimmed of Illumina adapters and low-quality (Q<20) nucleotides using TrimGalore (v0.6.7; ***Krueger, 2021***). Reads shorter than 15 bp were discarded. Trimmed reads were aligned to *Mus musculus* reference genome GRCm39 using HISAT2 (v2.2.1; ***Kim et al., 2019***). StringTie (v2.2.1; ***Kovaka et al., 2019***) was used to assemble genes and calculate gene abundance. Differential expression analysis was performed using DESeq2. Data was visualised using ShinyGo, ClustVis, Network Analyst, and Venny2.1 free web-based software using a padj<0.05, FDR<0.05, and no fold change cut-off. All gene expression data is publicly available via Gene Expression Omnibus (GSE301011).

Fetal sex determination

DNA was extracted from fetal tail tissue using the DNeasy Blood and Tissue Kit (QIAGEN, UK) according to the manufacturer's instructions. For PCR determination of fetal sex, 2 µl (100 ng) of template DNA was added to a mastermix comprising 10 µl mastermix (2×GoTaq Green Master Mix, Promega UK), 1 µl primer mix (25 µM forward and reverse primers), and 5 µl water per reaction. Amplification was performed using a Techgene thermocycler using three primer sets specific for regions on the Y (Sry and Zfy) and X (Dxnds3) chromosomes (primer sequences are provided in ***Supplementary file 2***).

Statistical analysis

All data were assessed for normality with GraphPad Prism (v10) or SPSS (v28). Early placental (EPC) data were analysed using a one-way ANOVA for normally distributed data or a Kruskal-Wallis test for non-normally distributed data with appropriate post hoc tests. For the analysis of stud male growth, an additional FDR correction was applied to account for the multiple testing of weight at each individual week. Late gestation (E17.5) fetal and placental data were analysed using a generalised linear mixed model analysis with paternal origin of litter and paternal duration on their respective diet incorporated as random effects (***Watkins et al., 2018***). Significance was taken at p<0.05.

Acknowledgements

The authors would like to thank the staff within the Bio Support Unit at the University of Nottingham for animal provision and maintenance. This work was supported by Biotechnology and Biological Sciences Research Council (BBSRC) grants (BB/R003556/1 and BB/V006711/1) to AJW. This work was also supported by a COVID support grant from the Society for Reproduction and Fertility awarded to NE. RTM was supported by a United Kingdom Research and Innovation (UKRI) Future Leaders Fellowship (MR/Y011783/1).

Additional information

Funding

Funder	Grant reference number	Author
Biotechnology and Biological Sciences Research Council	BB/R003556/1	Adam J Watkins
Biotechnology and Biological Sciences Research Council	BB/V006711/1	Adam J Watkins
United Kingdom Resarch and Innovation	Future Leaders Fellowship MR/Y011783/1	Rod T Mitchell

The funders had no role in study design, data collection and interpretation, or the decision to submit the work for publication.

Author contributions

Hannah L Morgan, Vipul Batra, Conceptualization, Data curation, Formal analysis, Investigation, Methodology, Writing – original draft, Writing – review and editing; Nader Eid, Nadine Holmes, Matthew Carlile, Sonal Henson, Fei Sang, Marcos Castellanos-Uribe, Iqbal Khan, Nazia Nazar, Federica Lopes, A Augusto Coppi, Conceptualization, Data curation, Formal analysis, Investigation, Methodology, Writing – review and editing; Victoria Wright, Sean T May, Robert S Robinson, Writing – review and editing; Rod T Mitchell, Conceptualization, Data curation, Formal analysis, Funding acquisition, Methodology, Writing – review and editing; Adam J Watkins, Conceptualization, Data curation, Formal analysis, Funding acquisition, Investigation, Methodology, Writing – original draft, Project administration, Writing – review and editing

Author ORCIDs

Sean T May https://orcid.org/0000-0001-5282-3250
Rod T Mitchell https://orcid.org/0000-0003-4650-3765
A Augusto Coppi https://orcid.org/0000-0002-8656-0409
Adam J Watkins https://orcid.org/0000-0002-0842-1251

Ethics

All animal procedures were conducted in accordance with the UK Home Office Animals (Scientific Procedures) Act 1986 and carried out under Project License PP8899264 with local ethical approval at University of Nottingham.

Peer review material

Version of Record:
Reviewer #1 (Public review): https://doi.org/10.7554/eLife.109392.4.sa1
Reviewer #2 (Public review): https://doi.org/10.7554/eLife.109392.4.sa2
Author response https://doi.org/10.7554/eLife.109392.4.sa3

Reviewed preprint v3
Reviewer #1 (Public review): https://doi.org/10.7554/eLife.109392.3.sa2
Reviewer #2 (Public review): https://doi.org/10.7554/eLife.109392.3.sa1
Author response: https://doi.org/10.7554/eLife.109392.3.sa0

Reviewed preprint v2
Reviewer #1 (Public review): https://doi.org/10.7554/eLife.109392.2.sa2
Reviewer #2 (Public review): https://doi.org/10.7554/eLife.109392.2.sa1
Author response: https://doi.org/10.7554/eLife.109392.2.sa0

Reviewed preprint v1
Reviewer #1 (Public review): https://doi.org/10.7554/eLife.109392.1.sa2
Reviewer #2 (Public review): https://doi.org/10.7554/eLife.109392.1.sa1
Author response: https://doi.org/10.7554/eLife.109392.1.sa0

Additional files

Supplementary files

Supplementary file 1. Ingredients and nutritional information of diets fed to male mice.

Supplementary file 2. Sexing PCR primer sequences.

Supplementary file 3. Late gestation placental RNA-seq data showing sexually dimorphic genes between males and females of the same parental diet group.

MDAR checklist

Data availability

All data are either contained within the supplementary files or have been deposited with in the Gene Expression Omnibus under accession numbers GSE301011 and GSE279868 respectively.

The following datasets were generated:

Author(s)	Year	Dataset title	Dataset URL	Database and Identifier
Morgan HL, Eid N, Holmes N, Carlile M, Henson S, Sang F, Wright V, Castellanos-Uribe M, Khan I, Nazar N, May ST, Mitchel RT, Lopes F, Robinson RS, Augusto Coppi A, Sturmey RG, Batra V, Watkins AJ	2025	Paternal over- and under-nutrition program fetal and placental development in a sex-specific manner	https://www.ncbi.nlm.nih.gov/geo/query/acc.cgi?acc=GSE301011	NCBI Gene Expression Omnibus, GSE301011
Eid N, Batra V, Holmes N, Carlile M, Henson S, Sang F, Wright V, Castellanos-Uribe M, Khan I, Nazar N, May ST, Mitchell RT, Lopes F, Robinson RS, Morgan HL, Watkins AJ	2025	Male metabolic and reproductive health are perturbed by both under- and over-nutrition in mice	https://www.ncbi.nlm.nih.gov/geo/query/acc.cgi?acc=GSE279868	NCBI Gene Expression Omnibus, GSE279868

References

Ajuogu PK, Al-Aqbi MA, Hart RA, Wolden M, Smart NA, McFarlane JR. 2020. The effect of dietary protein intake on factors associated with male infertility: a systematic literature review and meta-analysis of animal clinical trials in rats. *Nutrition and Health* **26**:53–64. DOI: https://doi.org/10.1177/0260106019900731, PMID: 31992124

Batra V, Norman E, Morgan HL, Watkins AJ. 2022. Parental programming of offspring health: the intricate interplay between diet, environment, reproduction and development. *Biomolecules* **12**:1289. DOI: https://doi.org/10.3390/biom12091289, PMID: 36139133

Bodden C, Pang TY, Feng Y, Mridha F, Kong G, Li S, Watt MJ, Reichelt AC, Hannan AJ. 2022. Intergenerational effects of a paternal Western diet during adolescence on offspring gut microbiota, stress reactivity, and social behavior. *FASEB Journal* **36**:e21981. DOI: https://doi.org/10.1096/fj.202100920RR, PMID: 34907601

Braun AE, Muench KL, Robinson BG, Wang A, Palmer TD, Winn VD. 2021. Examining sex differences in the human placental transcriptome during the first fetal androgen peak. *Reproductive Sciences* **28**:801–818. DOI: https://doi.org/10.1007/s43032-020-00355-8, PMID: 33150487

Broere-Brown ZA, Baan E, Schalekamp-Timmermans S, Verburg BO, Jaddoe VWV, Steegers EAP. 2016. Sex-specific differences in fetal and infant growth patterns: a prospective population-based cohort study. *Biology of Sex Differences* **7**:65. DOI: https://doi.org/10.1186/s13293-016-0119-1, PMID: 27980713

Brykczynska U, Hisano M, Erkek S, Ramos L, Oakeley EJ, Roloff TC, Beisel C, Schübeler D, Stadler MB, Peters A. 2010. Repressive and active histone methylation mark distinct promoters in human and mouse spermatozoa. *Nature Structural & Molecular Biology* **17**:679–687. DOI: https://doi.org/10.1038/nsmb.1821

Buckberry S, Bianco-Miotto T, Bent SJ, Dekker GA, Roberts CT. 2014. Integrative transcriptome meta-analysis reveals widespread sex-biased gene expression at the human fetal-maternal interface. *Molecular Human Reproduction* **20**:810–819. DOI: https://doi.org/10.1093/molehr/gau035

Cannarella R, Calogero AE, Condorelli RA, Greco EA, Aversa A, La Vignera S. 2021. Is there a role for glucagon-like peptide-1 receptor agonists in the treatment of male infertility? *Andrology* **9**:1499–1503. DOI: https://doi.org/10.1111/andr.13015, PMID: 33818920

Cao Q-F, Yamamoto J, Isobe T, Tateno S, Murase Y, Chen Y, Handa H, Yamaguchi Y. 2015. Characterization of the human transcription elongation factor Rtf1: evidence for nonoverlapping functions of Rtf1 and the Paf1 complex. *Molecular and Cellular Biology* **35**:3459–3470. DOI: https://doi.org/10.1128/MCB.00601-15

Capobianco E, Pirrone I. 2023. Paternal programming of fetoplacental and offspring metabolic disorders. *Placenta* **141**:71–77. DOI: https://doi.org/10.1016/j.placenta.2023.06.009, PMID: 37355440

Caporaso JG, Kuczynski J, Stombaugh J, Bittinger K, Bushman FD, Costello EK, Fierer N, Peña AG, Goodrich JK, Gordon JI, Huttley GA, Kelley ST, Knights D, Koenig JE, Ley RE, Lozupone CA, McDonald D, Muegge BD, Pirrung M, Reeder J, et al. 2010. QIIME allows analysis of high-throughput community sequencing data. *Nature Methods* **7**:335–336. DOI: https://doi.org/10.1038/nmeth.f.303

César H, Sertorio MN, de Souza EA, Jamar G, Santamarina A, Jucá A, Casagrande BP, Pisani LP. 2022. Parental high-fat high-sugar diet programming and hypothalamus adipose tissue axis in male Wistar rats. *European Journal of Nutrition* **61**:523–537. DOI: https://doi.org/10.1007/s00394-021-02690-1, PMID: 34657184

Colldén H, Landin A, Wallenius V, Elebring E, Fändriks L, Nilsson ME, Ryberg H, Poutanen M, Sjögren K, Vandenput L, Ohlsson C. 2019. The gut microbiota is a major regulator of androgen metabolism in intestinal contents. *American Journal of Physiology-Endocrinology and Metabolism* **317**:E1182–E1192. DOI: https://doi.org/10.1152/ajpendo.00338.2019

Cordero P, Campion J, Milagro FI, Martinez JA. 2013a. Transcriptomic and epigenetic changes in early liver steatosis associated to obesity: effect of dietary methyl donor supplementation. *Molecular Genetics and Metabolism* **110**:388–395. DOI: https://doi.org/10.1016/j.ymgme.2013.08.022, PMID: 24084163

Cordero P, Gomez-Uriz AM, Campion J, Milagro FI, Martinez JA. 2013b. Dietary supplementation with methyl donors reduces fatty liver and modifies the fatty acid synthase DNA methylation profile in rats fed an obesogenic diet. *Genes & Nutrition* **8**:105–113. DOI: https://doi.org/10.1007/s12263-012-0300-z

Crean AJ, Afrin S, Niranjan H, Pulpitel TJ, Ahmad G, Senior AM, Freire T, Mackay F, Nobrega MA, Barrès R, Simpson SJ, Pini T. 2023 Male reproductive traits are differentially affected by dietary macronutrient balance but unrelated to adiposity. *Nature Communications* **14**:38314-x. DOI: https://doi.org/10.1038/s41467-023-38314-x

Cui L, Nie X, Guo Y, Ren P, Guo Y, Wang X, Li R, Hotaling JM, Cairns BR, Guo J. 2025. Single-cell transcriptomic atlas of the human testis across the reproductive lifespan. *Nature Aging* **5**:658–674. DOI: https://doi.org/10.1038/s43587-025-00824-2, PMID: 40033047

Cvitic S, Longtine MS, Hackl H, Wagner K, Nelson MD, Desoye G, Hiden U. 2013. The human placental sexome differs between trophoblast epithelium and villous vessel endothelium. *PLOS ONE* **8**:e79233. DOI: https://doi.org/10.1371/journal.pone.0079233

Dearden L, Bouret SG, Ozanne SE. 2018. Sex and gender differences in developmental programming of metabolism. *Molecular Metabolism* **15**:8–19. DOI: https://doi.org/10.1016/j.molmet.2018.04.007, PMID: 29773464

de la Garza AL, Martínez-Tamez AM, Mellado-Negrete A, Arjonilla-Becerra S, Peña-Vázquez GI, Marín-Obispo LM, Hernández-Brenes C. 2022. Characterization of the cafeteria diet as simulation of the human western diet and its impact on the lipidomic profile and gut microbiota in obese rats. *Nutrients* **15**:86. DOI: https://doi.org/10.3390/nu15010086, PMID: 36615745

Fan Y, Liu Y, Xue K, Gu G, Fan W, Xu Y, Ding Z. 2015. Diet-induced obesity in male C57BL/6 mice decreases fertility as a consequence of disrupted blood-testis barrier. *PLOS ONE* **10**:e0120775. DOI: https://doi.org/10.1371/journal.pone.0120775

Fleming TP, Watkins AJ, Velazquez MA, Mathers JC, Prentice AM, Stephenson J, Barker M, Saffery R, Yajnik CS, Eckert JJ, Hanson MA, Forrester T, Gluckman PD, Godfrey KM. 2018. Origins of lifetime health around the time of conception: causes and consequences. *The Lancet* **391**:1842–1852. DOI: https://doi.org/10.1016/S0140-6736(18)30312-X

Fujinoki M. 2011. Serotonin-enhanced hyperactivation of hamster sperm. *Reproduction* **142**:255–266. DOI: https://doi.org/10.1530/REP-11-0074

Furse S, Morgan HL, Koulman A, Watkins AJ. 2023. Characterisation of the paternal influence on intergenerational offspring cardiac and brain lipid homeostasis in mice. *International Journal of Molecular Sciences* **24**:1814. DOI: https://doi.org/10.3390/ijms24031814, PMID: 36768137

Gao Y, Zhou Y, Hong Z, Ma B, Wang X, Nie L, Ma L, Zhang Y, Zhang M, Wang M. 2026. The intricate dance of RNA-binding proteins: unveiling the mechanisms behind male infertility. *Human Reproduction Update* **32**:58–104. DOI: https://doi.org/10.1093/humupd/dmaf023

Ghosh S, Mukherjee S. 2018. Testicular germ cell apoptosis and sperm defects in mice upon long-term high fat diet feeding. *Journal of Cellular Physiology* **233**:6896–6909. DOI: https://doi.org/10.1002/jcp.26581, PMID: 29665058

Gomes AC, Hoffmann C, Mota JF. 2020. Gut microbiota is associated with adiposity markers and probiotics may impact specific genera. *European Journal of Nutrition* **59**:1751–1762. DOI: https://doi.org/10.1007/s00394-019-02034-0

Gonzalez TL, Sun T, Koeppel AF, Lee B, Wang ET, Farber CR, Rich SS, Sundheimer LW, Buttle RA, Chen YDI, Rotter JI, Turner SD, Williams J III, Goodarzi MO, Pisarska MD. 2018. Sex differences in the late first trimester human placenta transcriptome. *Biology of Sex Differences* **9**:0165-y. DOI: https://doi.org/10.1186/s13293-018-0165-y

Hammoud SS, Nix DA, Hammoud AO, Gibson M, Cairns BR, Carrell DT. 2011. Genome-wide analysis identifies changes in histone retention and epigenetic modifications at developmental and imprinted gene loci in the sperm of infertile men. *Human Reproduction* **26**:2558–2569. DOI: https://doi.org/10.1093/humrep/der192

Hao Y, Feng Y, Yan X, Chen L, Zhong R, Tang X, Shen W, Sun Q, Sun Z, Ren Y, Zhang H, Zhao Y. 2022. Gut microbiota-testis axis: FMT improves systemic and testicular micro-environment to increase semen quality in type 1 diabetes. *Molecular Medicine* **28**:00473-w. DOI: https://doi.org/10.1186/s10020-022-00473-w

Howard V, Reed MG, Netlibrary I. 2005. *Unbiased Stereology: Three-Dimensional Measurement in Microscopy*. Garland Science/BIOS Scientific Publishers.

Hu Y, Xu J, Sheng Y, Liu J, Li H, Guo M, Xu W, Luo Y, Huang K, He X. 2022. Pleurotus ostreatus ameliorates obesity by modulating the gut microbiota in obese mice induced by high-fat diet. *Nutrients* **14**:1868. DOI: https://doi.org/10.3390/nu14091868

Jawaid A, Jehle K-L, Mansuy IM. 2021. Impact of parental exposure on offspring health in humans. *Trends in Genetics* **37**:373–388. DOI: https://doi.org/10.1016/j.tig.2020.10.006

Jazwiec PA, Patterson VS, Ribeiro TA, Yeo E, Kennedy KM, Mathias PCF, Petrik JJ, Sloboda DM. 2022. Paternal obesity induces placental hypoxia and sex-specific impairments in placental vascularization and offspring metabolism. *Biology of Reproduction* **107**:574–589. DOI: https://doi.org/10.1093/biolre/ioac066

Kim D, Paggi JM, Park C, Bennett C, Salzberg SL. 2019. Graph-based genome alignment and genotyping with HISAT2 and HISAT-genotype. *Nature Biotechnology* **37**:907–915. DOI: https://doi.org/10.1038/s41587-019-0201-4

Kovaka S, Zimin AV, Pertea GM, Razaghi R, Salzberg SL, Pertea M. 2019. Transcriptome assembly from long-read RNA-seq alignments with StringTie2. *Genome Biology* **20**:1910-1. DOI: https://doi.org/10.1186/s13059-019-1910-1

Krueger F. 2021. TrimGalore. 0.6.7. Babraham Bioinformatics. https://www.bioinformatics.babraham.ac.uk/projects/trim_galore/

Lambrot R, Xu C, Saint-Phar S, Chountalos G, Cohen T, Paquet M, Suderman M, Hallett M, Kimmins S. 2013. Low paternal dietary folate alters the mouse sperm epigenome and is associated with negative pregnancy outcomes. *Nature Communications* **4**:ncomms3889. DOI: https://doi.org/10.1038/ncomms3889

Leisegang K, Udodong A, Bouic PJD, Henkel RR. 2014. Effect of the metabolic syndrome on male reproductive function: a case-controlled pilot study. *Andrologia* **46**:167–176. DOI: https://doi.org/10.1111/and.12060

Li Y, Wang Y, Tan Y-Q, Yue Q, Guo Y, Yan R, Meng L, Zhai H, Tong L, Yuan Z, Li W, Wang C, Han S, Ren S, Yan Y, Wang W, Gao L, Tan C, Hu T, Zhang H, et al. 2024. The landscape of RNA binding proteins in mammalian spermatogenesis. *Science* **386**:eadj8172. DOI: https://doi.org/10.1126/science.adj8172

Liao Y, Wang J, Jaehnig EJ, Shi Z, Zhang B. 2019. WebGestalt 2019: gene set analysis toolkit with revamped UIs and APIs. *Nucleic Acids Research* **47**:W199–W205. DOI: https://doi.org/10.1093/nar/gkz401

Liu Y, Zhao W, Gu G, Lu L, Feng J, Guo Q, Ding Z. 2014. Palmitoyl-protein thioesterase 1 (PPT1): an obesity-induced rat testicular marker of reduced fertility. *Molecular Reproduction and Development* **81**:55–65. DOI: https://doi.org/10.1002/mrd.22281, PMID: 24302477

Liu S, Qin P, Wang J. 2019. High-fat diet alters the intestinal microbiota in streptozotocin-induced type 2 diabetic mice. *Microorganisms* **7**:176. DOI: https://doi.org/10.3390/microorganisms7060176, PMID: 31208113

Lotti F, Corona G, Degli Innocenti S, Filimberti E, Scognamiglio V, Vignozzi L, Forti G, Maggi M. 2013. Seminal, ultrasound and psychobiological parameters correlate with metabolic syndrome in male members of infertile couples. *Andrology* **1**:229–239. DOI: https://doi.org/10.1111/j.2047-2927.2012.00031.x

Ludwig DS, Peterson KE, Gortmaker SL. 2001. Relation between consumption of sugar-sweetened drinks and childhood obesity: a prospective, observational analysis. *The Lancet* **357**:505–508. DOI: https://doi.org/10.1016/S0140-6736(00)04041-1

Luisi S, Florio P, Reis FM, Petraglia F. 2005. Inhibins in female and male reproductive physiology: role in gametogenesis, conception, implantation and early pregnancy. *Human Reproduction Update* **11**:123–135. DOI: https://doi.org/10.1093/humupd/dmh057

Lv S, Huang J, Luo Y, Wen Y, Chen B, Qiu H, Chen H, Yue T, He L, Feng B, Yu Z, Zhao M, Yang Q, He M, Xiao W, Zou X, Gu C, Lu R. 2024. Gut microbiota is involved in male reproductive function: a review. *Frontiers in Microbiology* **15**:1371667. DOI: https://doi.org/10.3389/fmicb.2024.1371667

Mbogning J, Nagy S, Pagé V, Schwer B, Shuman S, Fisher RP, Tanny JC. 2013. The PAF complex and prf1/rtf1 delineate distinct cdk9-dependent pathways regulating transcription elongation in fission yeast. *PLOS Genetics* **9**:e1004029. DOI: https://doi.org/10.1371/journal.pgen.1004029

McPherson NO, Fullston T, Kang WX, Sandeman LY, Corbett MA, Owens JA, Lane M. 2016. Paternal under-nutrition programs metabolic syndrome in offspring which can be reversed by antioxidant/vitamin food fortification in fathers. *Scientific Reports* **6**:27010. DOI: https://doi.org/10.1038/srep27010

Morgan HL, Ampong I, Eid N, Rouillon C, Griffiths HR, Watkins AJ. 2020a. Low protein diet and methyl-donor supplements modify testicular physiology in mice. *Reproduction* **159**:627–641. DOI: https://doi.org/10.1530/REP-19-0435

Morgan HL, Paganopoulou P, Akhtar S, Urquhart N, Philomin R, Dickinson Y, Watkins AJ. 2020b. Paternal diet impairs F1 and F2 offspring vascular function through sperm and seminal plasma specific mechanisms in mice. *The Journal of Physiology* **598**:699–715. DOI: https://doi.org/10.1113/JP278270

Morgan HL, Aljumah A, Rouillon C, Watkins AJ. 2021a. Paternal low protein diet and the supplementation of methyl-donors impact fetal growth and placental development in mice. *Placenta* **103**:124–133. DOI: https://doi.org/10.1016/j.placenta.2020.10.020

Morgan HL, Eid N, Holmes N, Henson S, Wright V, Coveney C, Winder C, O'Neil DM, Dunn WB, Boocock DJ, Watkins AJ. 2021b. Paternal undernutrition and overnutrition modify semen composition and preimplantation embryo developmental kinetics in mice. *BMC Biology* **22**:01992-0. DOI: https://doi.org/10.1186/s12915-024-01992-0

Morgan HL, Furse S, Dias IHK, Shabir K, Castellanos M, Khan I, May ST, Holmes N, Carlile M, Sang F, Wright V, Koulman A, Watkins AJ. 2022. Paternal low protein diet perturbs inter-generational metabolic homeostasis in a tissue-specific manner in mice. *Communications Biology* **5**:929. DOI: https://doi.org/10.1038/s42003-022-03914-8, PMID: 36075960

Moss JL, Harris KM. 2015. Impact of maternal and paternal preconception health on birth outcomes using prospective couples' data in Add Health. *Archives of Gynecology and Obstetrics* **291**:287–298. DOI: https://doi.org/10.1007/s00404-014-3521-0

NCD Risk Factor Collaboration (NCD-RisC). 2024. Worldwide trends in underweight and obesity from 1990 to 2022: a pooled analysis of 3663 population-representative studies with 222 million children, adolescents, and adults. *Lancet* **403**:1027–1050. DOI: https://doi.org/10.1016/S0140-6736(23)02750-2

Ng S-F, Lin RCY, Laybutt DR, Barres R, Owens JA, Morris MJ. 2010. Chronic high-fat diet in fathers programs β-cell dysfunction in female rat offspring. *Nature* **467**:963–966. DOI: https://doi.org/10.1038/nature09491

Nielsen JE, Lindegaard ML, Friis-Hansen L, Almstrup K, Leffers H, Nielsen LB, Rajpert-De Meyts E. 2010. Lipoprotein lipase and endothelial lipase in human testis and in germ cell neoplasms. *International Journal of Andrology* **33**:e207–e215. DOI: https://doi.org/10.1111/j.1365-2605.2009.00988.x, PMID: 19780863

Omote M, Wakimoto Y, Shibahara H. 2023. Possible role of 5-hydroxytryptamine (5-ht) receptor on human sperm motility regulation. *Cureus* **15**:e49530. DOI: https://doi.org/10.7759/cureus.49530

O'Neill S, O'Driscoll L. 2015. Metabolic syndrome: a closer look at the growing epidemic and its associated pathologies. *Obesity Reviews* **16**:1–12. DOI: https://doi.org/10.1111/obr.12229

Osei-Kumah A, Smith R, Jurisica I, Caniggia I, Clifton VL. 2011. Sex-specific differences in placental global gene expression in pregnancies complicated by asthma. *Placenta* **32**:570–578. DOI: https://doi.org/10.1016/j.placenta.2011.05.005

Ozanne SE, Fernandez-Twinn D, Hales CN. 2004. Fetal growth and adult diseases. *Seminars in Perinatology* **28**:81–87. DOI: https://doi.org/10.1053/j.semperi.2003.10.015

Penesova A, Bunt JC, Bogardus C, Krakoff J. 2010. Effect of paternal diabetes on pre-diabetic phenotypes in adult offspring. *Diabetes Care* **33**:1823–1828. DOI: https://doi.org/10.2337/dc10-0664

Pepin A-S, Lafleur C, Lambrot R, Dumeaux V, Kimmins S. 2022. Sperm histone H3 lysine 4 tri-methylation serves as a metabolic sensor of paternal obesity and is associated with the inheritance of metabolic dysfunction. *Molecular Metabolism* **59**:101463. DOI: https://doi.org/10.1016/j.molmet.2022.101463

Petropoulos S, Edsgärd D, Reinius B, Deng Q, Panula SP, Codeluppi S, Plaza Reyes A, Linnarsson S, Sandberg R, Lanner F. 2016. Single-Cell RNA-seq reveals lineage and x chromosome dynamics in human preimplantation embryos. *Cell* **165**:1012–1026. DOI: https://doi.org/10.1016/j.cell.2016.03.023

Pokholok DK, Hannett NM, Young RA. 2002. Exchange of RNA polymerase ii initiation and elongation factors during gene expression in vivo. *Molecular Cell* **9**:799–809. DOI: https://doi.org/10.1016/S1097-2765(02)00502-6

Ribeiro AACM, de Oliveira Lacerda PM, Pereira de Melo M, de Carvalho Balieiro JC, de Souza RR. 2008. Placental microstructure and efficiency in cloned bovines: a design-based stereological approach. *Cell and Tissue Research* **333**:105–114. DOI: https://doi.org/10.1007/s00441-008-0626-4

Rosenfeld CS. 2015. Sex-specific placental responses in fetal development. *Endocrinology* **156**:3422–3434. DOI: https://doi.org/10.1210/en.2015-1227, PMID: 26241064

Saklayen MG. 2018. The global epidemic of the metabolic syndrome. *Current Hypertension Reports* **20**:0812-z. DOI: https://doi.org/10.1007/s11906-018-0812-z

Sanchez-Garrido MA, Ruiz-Pino F, Velasco I, Barroso A, Fernandois D, Heras V, Manfredi-Lozano M, Vazquez MJ, Castellano JM, Roa J, Pinilla L, Tena-Sempere M. 2018. Intergenerational influence of paternal obesity on metabolic and reproductive health parameters of the offspring: male-preferential impact and involvement of kiss1-mediated pathways. *Endocrinology* **159**:1005–1018. DOI: https://doi.org/10.1210/en.2017-00705

Sedlmeier E-M, Brunner S, Much D, Pagel P, Ulbrich SE, Meyer HH, Amann-Gassner U, Hauner H, Bader BL. 2014. Human placental transcriptome shows sexually dimorphic gene expression and responsiveness to maternal dietary n-3 long-chain polyunsaturated fatty acid intervention during pregnancy. *BMC Genomics* **15**:941. DOI: https://doi.org/10.1186/1471-2164-15-941

Serino M, Luche E, Gres S, Baylac A, Bergé M, Cenac C, Waget A, Klopp P, Iacovoni J, Klopp C, Mariette J, Bouchez O, Lluch J, Ouarné F, Monsan P, Valet P, Roques C, Amar J, Bouloumié A, Théodorou V, et al. 2012. Metabolic adaptation to a high-fat diet is associated with a change in the gut microbiota. *Gut* **61**:543–553. DOI: https://doi.org/10.1136/gutjnl-2011-301012

Siklenka K, Erkek S, Godmann M, Lambrot R, McGraw S, Lafleur C, Cohen T, Xia J, Suderman M, Hallett M, Trasler J, Peters AHFM, Kimmins S. 2015. Disruption of histone methylation in developing sperm impairs offspring health transgenerationally. *Science* **350**:aab2006. DOI: https://doi.org/10.1126/science.aab2006

Silva DR, Werneck AO, Collings PJ, Fernandes RA, Barbosa DS, Ronque ERV, Sardinha LB, Cyrino ES. 2017. Family history of cardiovascular disease and parental lifestyle behaviors are associated with offspring cardiovascular disease risk markers in childhood. *American Journal of Human Biology* **29**:22995. DOI: https://doi.org/10.1002/ajhb.22995, PMID: 28295804

Singh SP, Misra B, Kar SK, Panigrahi MK, Misra D, Bhuyan P, Pattnaik K, Meher C, Agrawal O, Rout N, Swain M. 2015. Nonalcoholic fatty liver disease (NAFLD) without insulin resistance: Is it different? *Clinics and Research in Hepatology and Gastroenterology* **39**:482–488. DOI: https://doi.org/10.1016/j.clinre.2014.08.014

Sood R, Zehnder JL, Druzin ML, Brown PO. 2006. Gene expression patterns in human placenta. *PNAS* **103**:5478–5483. DOI: https://doi.org/10.1073/pnas.0508035103

Squazzo SL, Costa PJ, Lindstrom DL, Kumer KE, Simic R, Jennings JL, Link AJ, Arndt KM, Hartzog GA. 2002. The Paf1 complex physically and functionally associates with transcription elongation factors in vivo. *The EMBO Journal* **21**:1764–1774. DOI: https://doi.org/10.1093/emboj/21.7.1764

Stern C, Schwarz S, Moser G, Cvitic S, Jantscher-Krenn E, Gauster M, Hiden U. 2021. Placental endocrine activity: adaptation and disruption of maternal glucose metabolism in pregnancy and the influence of fetal sex. *International Journal of Molecular Sciences* **22**:12722. DOI: https://doi.org/10.3390/ijms222312722, PMID: 34884524

Sugiyama Y, Fujinoki M, Shibahara H. 2019. Effects of 5-hydroxytryptamine on spermatozoal hyperactivation and *in vitro* fertilization in mice. *Journal of Reproduction and Development* **65**:541–550. DOI: https://doi.org/10.1262/jrd.2019-082

Veras MM, Damaceno-Rodrigues NR, Caldini EG, Ribeiro AACM, Mayhew TM, Saldiva PHN, Dolhnikoff M. 2008. Particulate urban air pollution affects the functional morphology of mouse placenta1. *Biology of Reproduction* **79**:578–584. DOI: https://doi.org/10.1095/biolreprod.108.069591

von Frankenberg AD, Marina A, Song X, Callahan HS, Kratz M, Utzschneider KM. 2017. A high-fat, high-saturated fat diet decreases insulin sensitivity without changing intra-abdominal fat in weight-stable overweight and obese adults. *European Journal of Nutrition* **56**:431–443. DOI: https://doi.org/10.1007/s00394-015-1108-6

Watkins AJ, Lucas ES, Marfy-Smith S, Bates N, Kimber SJ, Fleming TP. 2015. Maternal nutrition modifies trophoblast giant cell phenotype and fetal growth in mice. *Reproduction* **149**:563–575. DOI: https://doi.org/10.1530/REP-14-0667

Watkins AJ, Sirovica S, Stokes B, Isaacs M, Addison O, Martin RA. 2017. Paternal low protein diet programs preimplantation embryo gene expression, fetal growth and skeletal development in mice. *Biochimica et Biophysica Acta (BBA) - Molecular Basis of Disease* **1863**:1371–1381. DOI: https://doi.org/10.1016/j.bbadis.2017.02.009

Watkins AJ, Dias I, Tsuro H, Allen D, Emes RD, Moreton J, Wilson R, Ingram RJM, Sinclair KD. 2018. Paternal diet programs offspring health through sperm- and seminal plasma-specific pathways in mice. *PNAS* **115**:10064–10069. DOI: https://doi.org/10.1073/pnas.1806333115

Wilkinson AL, Menelaou K, Rakoczy J, Tan XS, Watson ED. 2021. Disruption of folate metabolism causes poor alignment and spacing of mouse conceptuses for multiple generations. *Frontiers in Cell and Developmental Biology* **9**:723978. DOI: https://doi.org/10.3389/fcell.2021.723978

Yang D, Dai F, Yuan M, Zheng Y, Liu S, Deng Z, Tan W, Chen L, Zhang Q, Zhao X, Cheng Y. 2021. Role of transforming growth factor-β1 in regulating fetal-maternal immune tolerance in normal and pathological pregnancy. *Frontiers in Immunology* **12**:689181. DOI: https://doi.org/10.3389/fimmu.2021.689181

Yi C, Kitamura Y, Maezawa S, Namekawa SH, Cairns BR. 2025. ZBTB16/PLZF regulates juvenile spermatogonial stem cell development through an extensive transcription factor poising network. *Nature Structural & Molecular Biology* **32**:1213–1226. DOI: https://doi.org/10.1038/s41594-025-01509-5

Zhang P, Feng Y, Li L, Ge W, Yu S, Hao Y, Shen W, Han X, Ma D, Yin S, Tian Y, Min L, Sun Z, Sun Q, Zhang H, Zhao Y. 2021. Improvement in sperm quality and spermatogenesis following faecal microbiota transplantation from alginate oligosaccharide dosed mice. *Gut* **70**:222–225. DOI: https://doi.org/10.1136/gutjnl-2020-320992, PMID: 32303608